Numerical Multi-scale Methods

Bjorn Engquist
University of Texas at Austin and
Royal Institute of Technology, Stockholm

Summer school on Multiscale Modeling and Applications, August 7-12, 2006, Cargese (Corsica), France

Outline

1. The challenge of multi-scale problems
2. Modeling strategies
3. Analytic model reduction
4. Traditional numerical multi-scale methods
5. Heterogeneous multi-scale methods and analysis
6. Analysis
7. Applications
8. Computational issues

1. The challenge of multi-scale problems

It is often natural to define scales in a physical process.

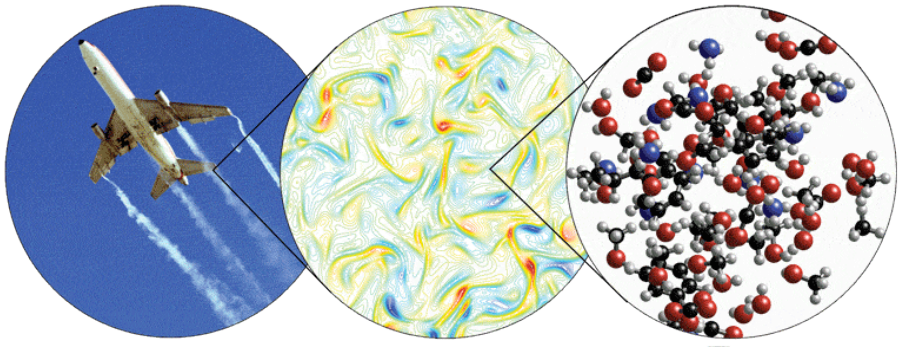

Examples of space scales are the size of the airplane, the turbulent eddies and the distance between the atoms. The time sales vary from the time of flight to the vibrations of the electrons. Different models are typically derived independently for the different scales. We will focus on problems where more than one scale and model is needed and where the micro-scale model is too computationally costly.

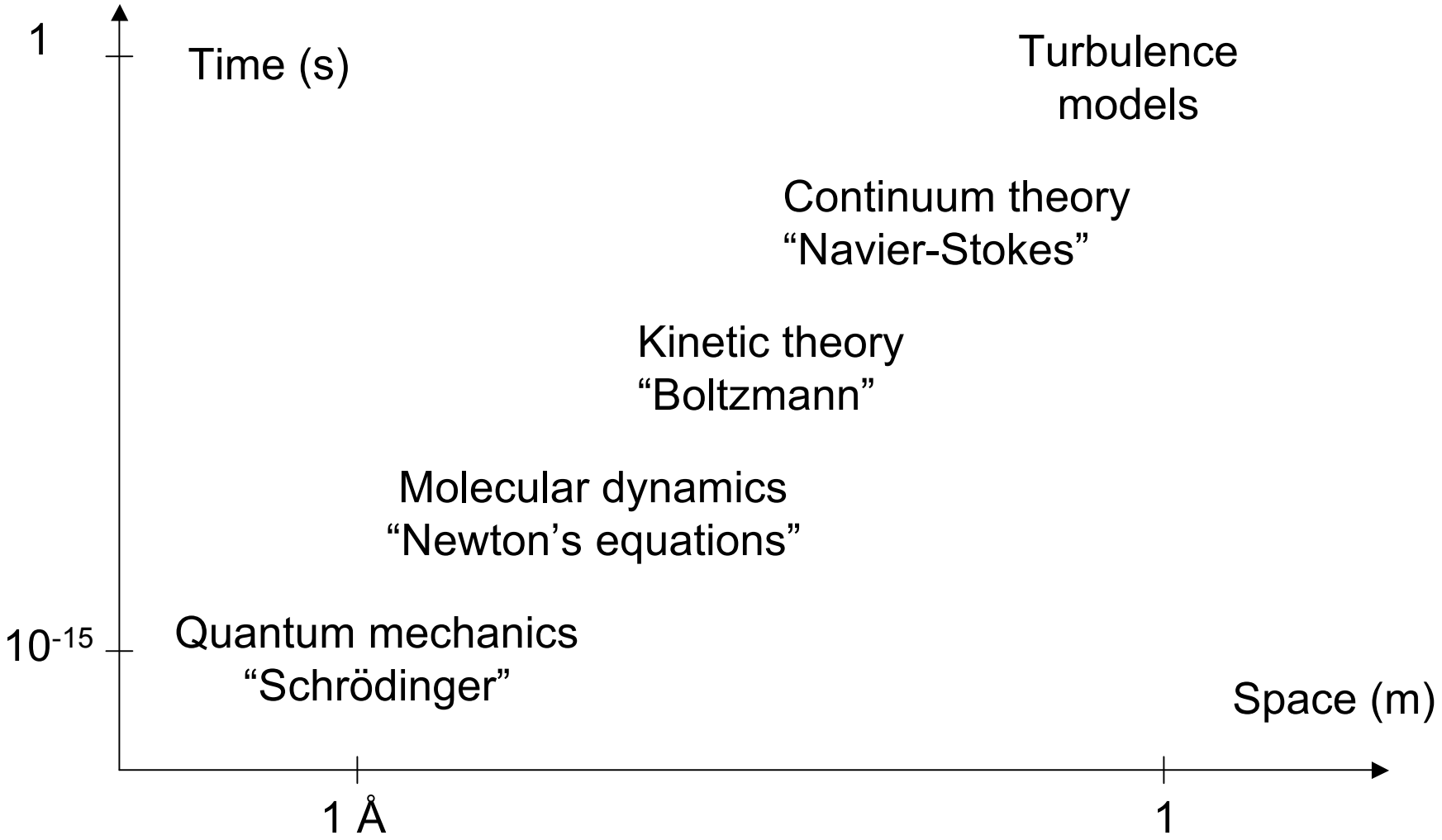
1
Time (s)
Turbulence
models
Continuum theory
“Navier-Stokes”
Kinetic theory
“Boltzmann”
Molecular dynamics
“Newton’s equations”
10-15
Quantum mechanics
“Schrödinger”
Space (m)
1 Å
1

1.1 Computational complexity

- A major reason for deriving effective equations with a narrow range of scales is the high computational cost of directly solving multi-scale problems.
- With the largest wavelength = L (the size of the computational domain) in each direction and the smallest wavelength = ε the typical number of operations in the solution of a multi-scale differential equation in d dimensions for a fixed prescribed accuracy is,

$$flop = O((N(\varepsilon/L)(\varepsilon/L)^{-1})^{dr}) = O((L/\varepsilon)^{\alpha}), \quad \alpha \geq d$$

$$\#\ unknowns \geq 2(L/\varepsilon)^{d} \quad [Shannon]$$

With L=1 we have,

$$flop = O((N(\varepsilon)\varepsilon^{-1})^{dr})$$

N(ε): number of unknowns per wavelength to achieve a given accuracy (*N(ε)≥2* from Shannon sampling theorem,

N(ε)≈ O(ε$^{-1/2}$) for standard second order finite difference methods). N typically scales as O(δ^{-s}), s>0, where δ is the prescribed accuracy

ε: the shortest wavelength to be approximated

d: number of dimensions

r: exponent for number of flops per unknown in the numerical method (r=1 for explicit methods and r=3 for Gaussian elimination of dense matrices)

Even with the best numerical methods:, r=1, N(ε) bounded,

$$flop = O(\varepsilon^{-d})$$

and this prohibits numerical simulation based on direct atomistic models over sizes in the millimeter range or more.

The upper limit for a teraflop computer is thus practically ε=10^{-4} with 10000 degrees of freedom in each dimension, R^{3+1}.

New approximate effective equations must be derived or the computation must be reduced to a small sample of the original domain.

For clarity in the presentation we will mainly consider "two-scale" problems: a macro-scale in the range of O(1) and a micro-scale with wave-lengths $O(\varepsilon)$ rather than full multi-scale problems.

When there is a continuum of scales we assume they are in the range $O(\varepsilon)$ to O(1).

We will typically be interested in macro-scale variables for which a higher fidelity of the micro-scale model is needed.

1.2 Two basic types of problems for which the macro-scale model fails

- Type A: Macro-scale model is accurate enough in most of computational domain Ω_1. Micro-scale model used in the complement Ω_2. Compare mesh refinement and heterogeneous domain decomposition.

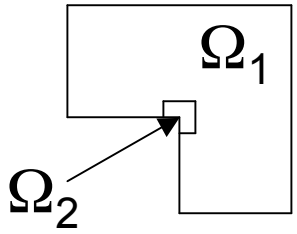

- Type B: A Macro-scale model is not fully known throughout computational domain. Sampling the micro-scale

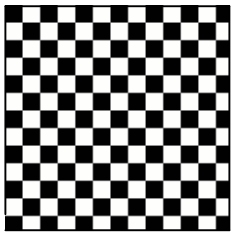

2. Modeling strategies

- Modeling: analytical and numerical models
- Analytical models
  - Purpose: find equations for appropriate range of scales
  - Use science, mathematics and experiments

    (Here mainly as background for understanding the numerical methods.)
- Numerical models
  - Purpose: increase computational efficiency and accuracy
  - Efficient algorithms and coupling of different models

Let us formally write the original multi-scale differential equation as,

$$F_\varepsilon(u_\varepsilon) = 0$$

where F_ε represents the differential equations with initial and boundary conditions. Analytically we are interested in finding $\bar{u}$ and effective $\bar{F}$ such that,

$$\lim_{\varepsilon \to 0} u_\varepsilon = \bar{u}$$

$$\bar{F}(\bar{u}) = 0$$

The topology for the weak or strong convergence will be different for different cases.

The scales could be given by the geometry or in the differential equations. In the Navier-Stokes equation the Reynolds number guides the nonlinear generation of a wide spectrum of scales. The Maxwell's equation is the same on atomistic and galactic scales and multi-scale effects comes from boundary conditions.

In our analysis we will define the scales more explicitly, for example, by a scaling law.

The function $f_\varepsilon(x) = f(x,x/\varepsilon)$, where $f(x,y)$ is 1-periodic in y, or where $f(x,y) \to F(x)$ as $y \to 0$, are said to contain the scales 1 and ε.

The scales are also naturally described by a scale-based transform of a function as, for example, Fourier or wavelet transforms.

Computational strategies

Let the equation below represent a multi-scale problem with range of scales O(ε) to O(1)

$$F_\varepsilon(u^\varepsilon) = 0$$

In the ideal case we can find an analytic model reduction which produces a model (effective or homogenized equation) with a narrow range of scales

$$F_\varepsilon(u^\varepsilon) = 0$$

$$\overline{F}(\overline{u}) = 0$$

This model can then be efficiently numerically approximated

$$F_\varepsilon(u^\varepsilon) = 0$$

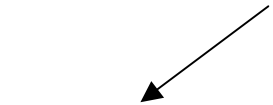

$$\overline{F}(\overline{u}) = 0$$

$$\overline{F}_h(\overline{u}_h) = 0$$

If appropriate effective equations are not available special numerical techniques are needed. With ε very small direct numerical simulation is too costly and a numerical model reduction is required

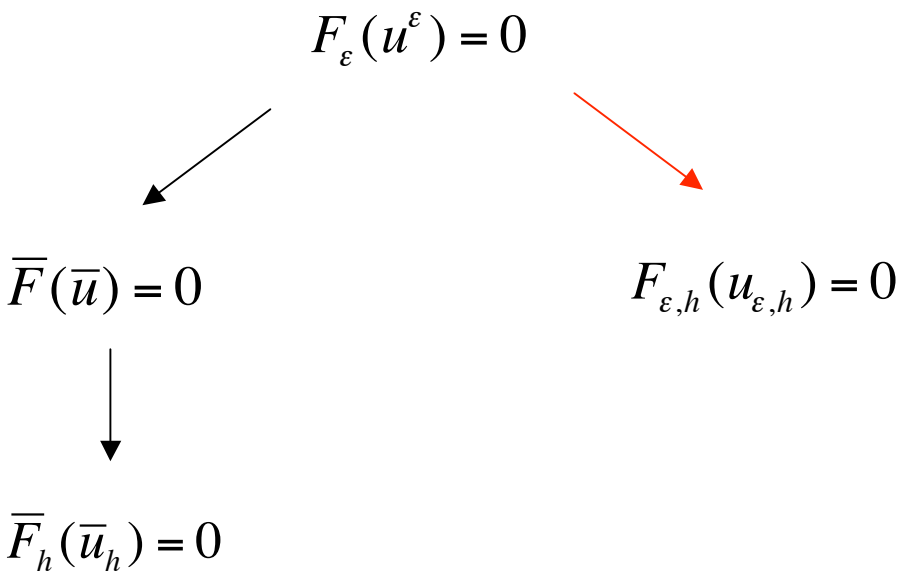

Standard numerical model reduction starts with direct numerical simulation model

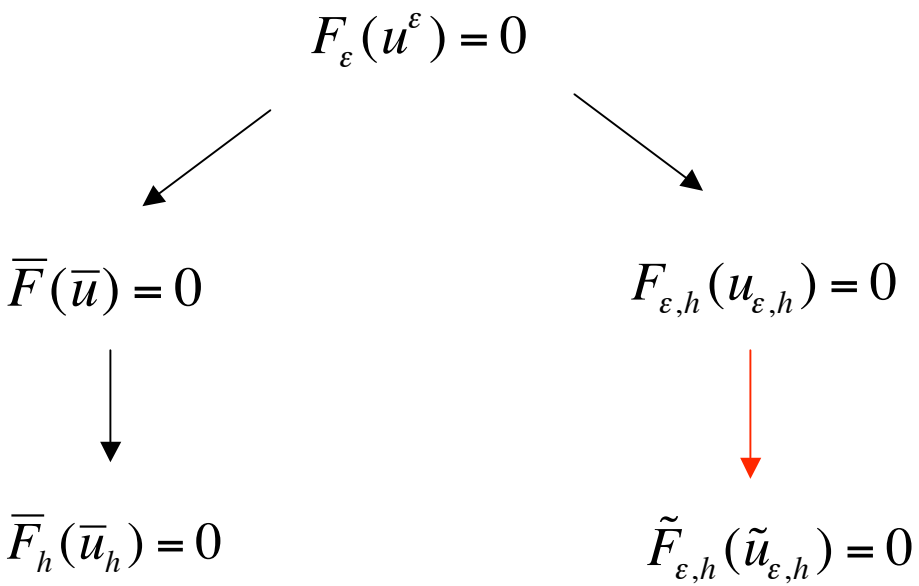

..but there are techniques that uses sampling and are influenced by analytic effective equations

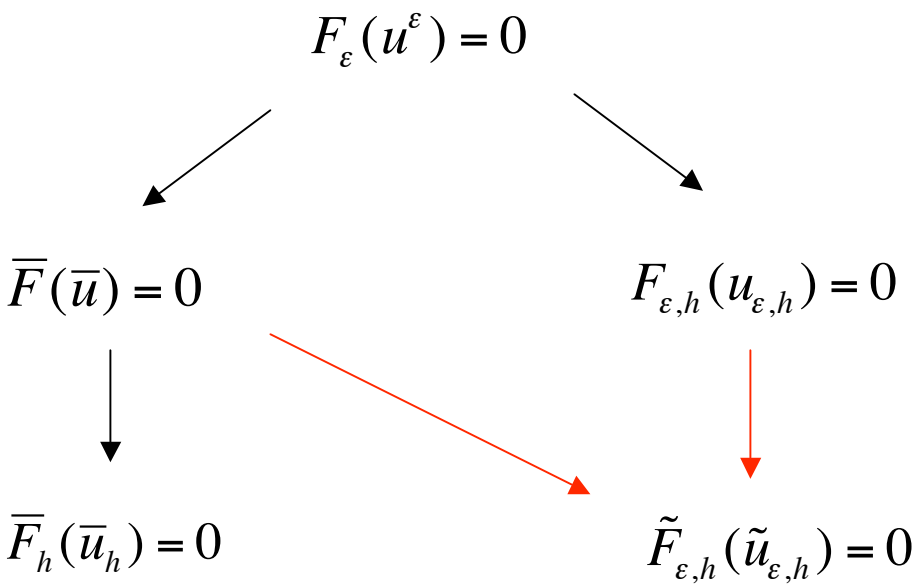

3. Analytic model reduction

- These techniques are often found in the physics, mechanics or in the classical applied mathematics literature and are commonly seen as part of these sciences rather than “just” mathematical techniques.
- A goal is to reduce a model with a broad range of scales to one with a narrow range. Such simpler models or effective equations are typically easier to analyze and better as basis for numerical simulation.
- Many times the different models for different ranges of scales are derived independently and the connection between the models developed later. Rigorous mathematical analysis connecting the models is often missing.

Examples of analytic techniques

Applied mathematics and mechanics related techniques

- Singular perturbations (✓)
- Stiff dynamical systems (✓)
- Homogenization methods (✓)
- Geometrical optics and geometrical theory of diffraction (✓)
- Boundary layer theory (✓)

Examples from theoretical physics

- Renormalization group methods
- Semi classical representation, path integral techniques, Wigner distributions
- Density function theory

3.1 Classical analytic techniques

We discussed briefly a number of mathematical techniques for deriving effective equations in 1.3. We will consider four of those in more detail and they are chosen to give representative examples of a variety of analytic techniques and will be used in connection to the numerical techniques later.

3.2 Singular perturbations of differential equations

3.3 Stiff ordinary differential equations

3.4 Homogenization of elliptic differential equations

3.5 Geometrical optics

Remark: Analytical reasoning is often the basis for numerical multi-scale methods

3.2 Singular perturbations

We will consider examples where the the micro scales are localized - a type A problem. The purpose is the derivation of the limiting effective equations and the study of the limiting process.

$$-\varepsilon \frac{d^2 u_\varepsilon}{dx^2} + a \frac{du_\varepsilon}{dx} + b u_\varepsilon = f(x) \quad 0 < x < 1$$

$$u_\varepsilon(0) = u_L, \quad u_\varepsilon(1) = u_R$$

$$\varepsilon, a, b > 0$$

The formal limit of this differential equation is of first order and only requires one boundary condition. In this case we can solve the original problem to see which boundary condition should be kept

$$u_\varepsilon = u_{ih} + u_h$$

$$u_{ih}(x) = \int_0^x \exp(-b/a(x-\xi) f(\xi) d\xi + O(\varepsilon)$$

$$u_h(x) = A_1 \exp(z_1 x) + A_2 \exp(z_2 x)$$

The inhomogeneous part of the solution u_{ih} is smooth as $\varepsilon \to 0$. The homogenous part u_h matches the boundary conditions resulting from u_{ih} with z_1 and z_2 the roots of the characteristic equation,

$$-\varepsilon z^2 + az + b = 0$$

$$z_1 = a/(2\varepsilon) + \sqrt{((a/(2\varepsilon))^2 - b}), \quad z_2 = a/(2\varepsilon) - \sqrt{((a/(2\varepsilon))^2 - b},$$

Recall the form of the homogeneous part,

$$u_h(x) = A_1 \exp(z_1 x) + A_2 \exp(z_2 x)$$
$$z_1 = a/\varepsilon + O(\varepsilon), \quad z_2 = \varepsilon/a + O(\varepsilon^3)$$

The coefficients A_1 and A_2 are determined to match the boundary conditions

$$A_1 + A_2 = -u_{ih}(0)$$
$$A_1 \exp(z_1) + A_2 \exp(z_2) = -u_{ih}(1)$$
$$A_1 \approx -u_{ih}(1)\exp(-z_1), \quad A_2 = -A_1$$

Thus u_{ih} is exponentially small in ε away from a boundary layer close to x=1.

The effective equation is

$$a\frac{du}{dx} + bu = f(x), \quad 0 < x < 1$$
$$u(0) = u_L$$

and u^ε converges to u point wise in any domain $0 \le x \le r < 1$, with the error $O(\varepsilon)$.

The inner solution and the boundary layer solution can be matched together to form an approximation for the full interval. This type of approximation goes under the name of matched asymptotics. One such example is the tripple deck method in fluid mechanics. Three approximating layers are matched.

Numerically we can use the reduced equation and a coarse grid for most of the domain away from x=1. “upwinding” keeps the correct influence from the boundary

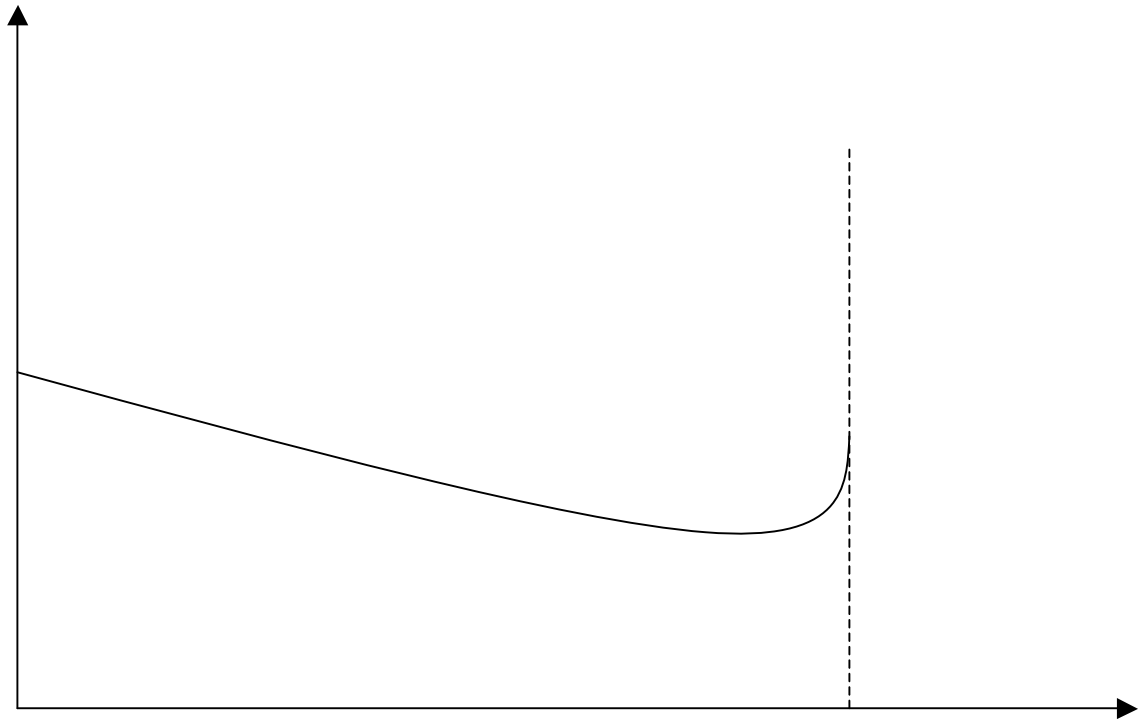

Prandtl boundary layer equations

One classical example of an effective boundary layer equation is the Prandtl equation as a limit of high Reynolds number Navier-Stokes equations,

$$\frac{\partial u}{\partial t} + u\frac{\partial u}{\partial x} + v\frac{\partial u}{\partial y} + \frac{\partial p}{\partial x} = \frac{1}{R}\left(\frac{\partial^2 u}{\partial x^2} + \frac{\partial^2 u}{\partial y^2}\right)$$

$$\frac{\partial v}{\partial t} + u\frac{\partial v}{\partial x} + v\frac{\partial v}{\partial y} + \frac{\partial p}{\partial y} = \frac{1}{R}\left(\frac{\partial^2 v}{\partial x^2} + \frac{\partial^2 v}{\partial y^2}\right)$$

$$\frac{\partial u}{\partial x} + \frac{\partial u}{\partial y} = 0, \quad y > 0, -\infty < x < \infty, t > 0,$$

$$u(x, y, 0), v(x, y, 0) \text{ given initial values},$$

$$u = v = 0, \quad y = 0, \quad -\infty < x < \infty,$$

The Prandtl assumption is that the inertia terms are balanced by the viscous terms in the a boundary layer of thickness δ (0<y< δ). Rescaling the independent variables $y/\delta \rightarrow \eta$ and using the divergence free condition,

$$\frac{\partial}{\partial y} \rightarrow \delta^{-1} \frac{\partial}{\partial \eta}, \quad \frac{\partial u}{\partial x} + \frac{\partial v}{\partial y} = 0$$

implies the scaling u=O(1), v=O(δ). Following the tradition we will use y for the new variable η and study the scaling of the terms in the original equations.

$$\frac{\partial u}{\partial t} + u\frac{\partial u}{\partial x} + v\frac{\partial u}{\partial y} + \frac{\partial p}{\partial x} = \frac{1}{R}\left(\frac{\partial^2 u}{\partial x^2} + \frac{\partial^2 u}{\partial y^2}\right)$$

$$1 \quad 1 \quad \delta\ \delta^{-1} \quad 1 \quad 1 \quad \delta^{-2}$$

Balancing inertia and viscous terms implies $R=O(\delta^{-2})$.

$$\frac{\partial v}{\partial t} + u\frac{\partial v}{\partial x} + v\frac{\partial v}{\partial y} + \frac{\partial p}{\partial y} = \frac{1}{R}\left(\frac{\partial^2 v}{\partial x^2} + \frac{\partial^2 v}{\partial y^2}\right)$$

$$\delta \quad \delta \quad \delta \quad \delta^{-1} \quad \delta^2 \quad \delta^2 \quad 1$$

Leading orders of δ in the second equation gives ,

$$\frac{\partial p}{\partial y} = 0 \quad \Rightarrow \quad p = P(x)$$

We then get the Prandtl boundary layer equation from the first equation,

$$\frac{\partial u}{\partial t} + u\frac{\partial u}{\partial x} + v\frac{\partial u}{\partial y} + P_x = \frac{\partial^2 u}{\partial y^2}$$

$$v = -\int_0^y \frac{\partial u}{\partial x} d\varsigma,$$

$$u(x,y,0) \; given \; initial \; values$$

$$u(x,0,t) = 0, \; u(x,1,t) = U(x,t)$$

3.3 Stiff dynamical systems

Analysis of certain types of stiff dynamical systems resembles that of singular perturbations above. A system of ordinary differential equations is said to be stiff if the eigenvalues of the matrix A below are of strongly different magnitude or if the magnitude of the eigenvalues are large compared to the length of interval of the independent variable,

$$\frac{du}{dt} = Au + f(t), \quad t > 0, \quad u : R^1 \rightarrow R^d$$
$$u(0) = u_0$$

The following nonlinear system is stiff for $0 < \varepsilon << 1$,

$$\frac{du_\varepsilon}{dt} = f(u_\varepsilon, v_\varepsilon),$$
$$\frac{dv_\varepsilon}{dt} = \varepsilon^{-1} g(u_\varepsilon, v_\varepsilon), \quad t > 0$$
$$u_\varepsilon(0) = u_0, v_\varepsilon(0) = v_0$$

If the conditions below are valid it has resemblance to the singular perturbation case,

$$\mathrm{Re}(\sigma(\frac{\partial g}{\partial v_\varepsilon})) \le \bar{\lambda} < 0, \quad \det(\frac{\partial g}{\partial u_\varepsilon}) \neq 0$$

From

$$\frac{du_\varepsilon}{dt} = f(u_\varepsilon, v_\varepsilon),$$
$$\frac{dv_\varepsilon}{dt} = \varepsilon^{-1} g(u_\varepsilon, v_\varepsilon)$$

We have the differential algebraic equations (DAE),

$$u_\varepsilon(t) \to u(t), v_\varepsilon(t) \to v(t), \quad t \geq \bar{t} > 0, as\ \varepsilon \to 0,$$
$$\frac{\partial u}{\partial t} = f(u,v), \quad u(0) = u_0$$
$$g(u,v) = 0, \quad defines\ v$$

The original functions have an exponential transient of order O(1) right after t=0 before converging to (u,v). The reduced system represents the slow manifold of the solutions of the original system.

Compare the Born-Oppenheimer approximation and the numerical Car-Parinello method.

Oscillatory solutions

- For nonlinear problems simple averaging does not work
  <f(u)> ≠ f(<x>).
- Averaging must take resonance into account. This is possible for polynomial f.
- A typical application is finite temperature molecular dynamics.
- Simple oscillatory example (that we will use later),

$$\frac{du}{dt} = \varepsilon^{-1} v, \quad \frac{dv}{dt} = -\varepsilon^{-1} u, \quad \frac{dw}{dt} = u^2 + v^2,$$

$$u(0) = 0, v(0) = 1, w(0) = 0$$

$$\Rightarrow u(t) = \sin(t/\varepsilon), v(t) = \cos(t/\varepsilon), w(t) = t$$

3.4 Homogenization

Homogenization is an analytic technique that applies to a wide class of multi-scale differential equations. It is used for analysis and for derivation of effective equations.

Let us start with the example of a simple two-point boundary value problem where a_ε may represent a particular property in a composite material.

$$\frac{d}{dx}\left(a_\varepsilon(x)\frac{du_\varepsilon}{dx}\right) = f(x), \quad 0 < x < 1,$$

$$u_\varepsilon(0) = u_\varepsilon(1) = 0$$

$$a_\varepsilon(x) = a(x/\varepsilon) > 0$$

The high frequencies in a_ε interact with those in $\frac{du_\varepsilon}{dx}$ to create low frequencies.

If we assume $a(y)$ to be 1-periodic then $a(x/\varepsilon)$ is highly oscillatory with wave length ε. The oscillations in a_ε will create oscillations in the solution u_ε. The oscillations in a_ε and u_ε interact to create low frequencies from these high frequencies. The effective equations can not simply be derived by taking the arithmetic average of a_ε.

This example can be analyzed by explicitly deriving the solution. After integration of the differential equation we have

$$a_\varepsilon(x)\frac{du_\varepsilon}{dx} = \int_0^x f(\xi)d\xi + C$$

$$u_\varepsilon(x) = \int_0^x (a_\varepsilon(\xi)^{-1}(\int_0^\xi f(\eta)d\eta + C)d\xi$$

The constant C is determined by the boundary conditions,

$$0 = \int_0^1 (a_\varepsilon(\xi)^{-1}(\int_0^\xi f(\eta)d\eta + C))d\xi$$

$$C = -\int_0^1 (a_\varepsilon(\xi)^{-1}\int_0^\xi f(\eta)d\eta)d\xi / \int_0^1 (a_\varepsilon(\xi)^{-1}\xi d\xi$$

In this explicit form of the solution it is possible to take the limit as $\varepsilon \to 0$.

$$\lim_{\varepsilon\to 0}\int_0^x (a(\xi/\varepsilon)^{-1}F(\xi)d\xi = \int_0^1 a(y)^{-1}dy \int_0^x F(\xi)d\xi, \quad F \in C[0,1]$$

$$define \quad \tilde{a} = \left(\int_0^1 a(y)^{-1}dy\right)^{-1}$$

$$\tilde{a}\frac{\partial^2 u}{\partial x^2} = f(x), \qquad u_\varepsilon \to u \quad as\ \varepsilon \to 0$$

Elliptic homogenization problems

For most problems there is no closed form solution and the procedure in our simple example cannot be followed.

The typical approach in to assume an expansion of the solution in terms of a small parameter ε, insert the expansion into the differential equation and then to find some closure process to achieve the convergence result and the effective equation.

$$-\nabla \cdot (a(x, x/\varepsilon)\nabla u_\varepsilon(x)) + a_0(x, x/\varepsilon)u_\varepsilon(x) = f(x), \quad x \in \Omega$$

$$u_\varepsilon(x) = 0, \quad x \in \partial\Omega \; boundary \; of \; \Omega \subset R^d$$

Assume the matrix $a(x,y)$ to be positive definite and 1-periodic in y,
The function $a_0(x,y)$ is also assumed to be positive and 1-periodic in y.
The asymptotic assumption on u_ε is as follows,

$$u_\varepsilon(x) = u_0(x, x/\varepsilon) + \varepsilon u_1(x, x/\varepsilon) + \varepsilon^2 u_2(x, x/\varepsilon) + \ldots$$

$$u_j(x, y), \quad 1 - periodic \; in \; y, \quad j = 1, 2, \ldots$$

Introduce the variable $y=x/\varepsilon$ and equate the different orders of ε. The equation for the ε^{-2} terms is

$$-\nabla_y a(x,y)\nabla_y u_0(x,y) = 0$$

with periodic boundary conditions in y. This implies

$$u_0(x,y) = u(x)$$

The equation for the ε^{-1} terms gives a representation of u_1 in terms of u. The terms of order O(1), O(ε), etc. couple the unknown terms in the expansion of u_ε but the closure assumption that $u_2(x,y)$ is 1-periodic in y generates the effective equation as conditions on u for existence of u_2.

The effective or homogenized equations take the form,

$$-\nabla A(x)\nabla u(x) + \bar{a}(x)u(x) = f(x)$$

$$A : a_{ij}(x) = \frac{1}{|T|}\int_T (a_{ij}(x,y) + a_{ik}\frac{\partial \kappa^j(x,y)}{\partial y_k})dy$$

$$\bar{a}(x) = \frac{1}{|T|}\int_T a_0(x,y)dy$$

The function κ is a solution of the cell problem,

$$-(\frac{\partial}{\partial y_i}a_{ik}(x,y))\frac{\partial \kappa^j}{\partial y_k}) = -\frac{\partial a_{ij}(x,y)}{\partial y_i}$$

$$\kappa \text{ periodic bc in } y$$

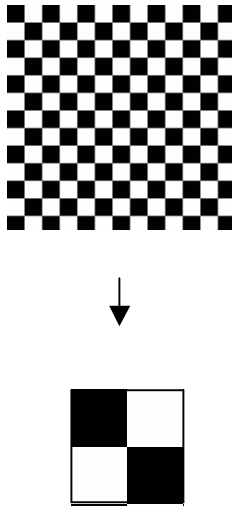

3.5 Geometrical optics

Geometrical optics equations are effective equations for high frequency wave propagation. Instead of approximating highly oscillatory functions geometrical optics gives the phase $\phi(x,t)$ and amplitude $A(x,t)$.

In this case the effective formulation were known long before the wave equation form.

New variables are introduced and not just the strong or weak limit of the original dependent variables.

Scalar wave equation

$$\frac{\partial u^2(x.t)}{\partial t^2} = c(x)^2 \Delta u(x,t)$$

$$u(x,0) = u_0(x), \quad \frac{\partial u(x,0)}{\partial t} = u_1(x)$$

The velocity is denoted by *c* and the initial values are assumed to be highly oscillatory such that the following form is appropriate,

$$u(x,t) = \exp(i\omega\varphi(x,t)) \sum_{\omega=0}^{\infty} A_j(x,t)\omega^{-j}, \quad \omega >> 1$$

Insert the expansion into the wave equation and equate the different orders of ω ($=\varepsilon^{-1}$). The leading equations give the eikonal and transport equations where there is no ω,

$$\frac{\partial \varphi}{\partial t} + c(x)\left|\nabla \varphi\right| = 0, \quad (\left|\cdot\right| = \textit{Euclidean norm})$$

$$\frac{\partial A_0}{\partial t} + c(x)\frac{\nabla \varphi \cdot \nabla A_0}{\left|\nabla \varphi\right|} + \frac{c(x)^2 \Delta \varphi - \dfrac{\partial^2 \varphi}{\partial t^2}}{2c(x)\left|\nabla \varphi\right|} A_0 = 0$$

The traditional ray tracing can be seen as the method of characteristics applied to the eikonal equation,

$$\frac{dx}{dt} = \nabla_p H(x,p), \quad \frac{dp}{dt} = \nabla_x H(x.p)$$

$$H(x.p) = c(x)\left|p\right|$$

4. Reduced complexity in numerical methods

- These techniques are used when appropriate effective equations are not known
- Fast methods resolving all scales (complexity $\rightarrow O(\varepsilon^{-d})$)
  - High order methods reducing number of unknowns
  - Traditional multi -scale methods: multi-grid, fast multi-pole (using special features in operator)
  - Can not be used for extreme ε
- Numerical model reduction methods starting with all scales resolved
  - Multi-scale finite element methods (MSFEM)
  - Wavelet based model reduction
  - Can not be used for extreme ε
- Fast methods not resolving all scales (using special features in solution, i.e. scale separation)

4.1 Traditional numerical multi-scale methods

- The multigrid methods aims at solving the fully discretized problem

$$F_{\varepsilon,h}(u_{\varepsilon,h}) = 0$$

  by reducing the computational complexity over direct methods for solving linear systems: r=1 in

$$flop = O((N(\varepsilon)\varepsilon^{-1})^{dr})$$

- A hierarchy of different grids is used in this iterative method. The different grids focus on different scales. The analytic properties of the differential equation is taken advantage of. Smoothing is essential.

- The analytic properties of the original problem is also important for the fast multy-pole method (FMM)
- Hierarchical domain decomposition
- Conjugate gradient type of methods

4.2 Numerical model reduction

We will briefly consider two classes of methodologies:

- Standard model reduction of input-output systems as in control theory
- Model reduction using compression and special basis functions

Remark. The computational cost of using these methods is at least as large as the solution of the original full system. The gain comes from the potential of using the same reduced system for a large set of inputs.

Standard model reduction

Consider the input-output system

$$\frac{dx(t)}{dt} = Ax(t) + Bu(t), \quad x \in R^n, u \in R^m$$
$$y(t) = Cx(t) + Du(t), \quad y \in R^p$$

The matrix A may be the result of a spatial discretization and the dimension n is assumed to be much larger than m and p.

Transient and filtered modes are eliminated to produce an approximation with lower dimensional A. SVD of A is a possible technique. Different methods are found in the control literature.

Special basis functions

We will briefly consider two examples: the multi-scale finite element method (MSFEM) [Hou] and wavelet based homogenization [E., Runborg]

In MSFEM the basis functions that are used in the finite element method are chosen to satisfy the homogeneous form of the original multi-scale problem.

The wavelets in wavelet based homogenization are used to keep the reduced operators sparse during the computation. A discretized differential equation equation in a wavelet basis is reduced by Schur complement

$$\begin{pmatrix} A_{11} & A_{12} \\ A_{21} & A_{22} \end{pmatrix} \begin{pmatrix} u_H \\ u_L \end{pmatrix} = \begin{pmatrix} f_H \\ f_L \end{pmatrix} \quad \rightarrow \quad (A_{22} - A_{21}A_{11}^{-1}A_{12})u_L = f_l - A_{21}A_{11}^{-1}f_H$$

5. Heterogeneous multi-scale methods

The heterogeneous multi-scale method (HMM) is a framework for developing and analyzing computational multi-scale models. A macro-scale method is coupled to a micro-scale method. The micro-scale technique is only applied in part of the computational domain

The coupling is based on related theory for analysis of effective equations. The gain in efficiency over applying the micro-scale method everywhere follows from the application of the micro-scale model only in sampled domains.

In collaboration with Weian E. [E. W., B. Engquist, The heterogeneous multi-scale method, Comm. Mat, Science, 1, 87-133, 2003]

The HMM framework

- Design macro-scale scheme for the desired variables. The scheme may not be valid in all of the computational domain (type A) or components of the scheme may not be known in full domain (type B).
- Use micro-scale numerical simulations to supply missing data in macro-scale model

Examples of other "better than $O(\varepsilon^{-d})$" multi-scale methods based on sampling

- Quasi continuum method
- Ultra FFTs
- Equation-free computation
- Gas kinetic schemes
- Super-parametrization

The quasi continuum method

- Coupling of molecular dynamics and continuum mechanics for zero temperature simulations
- Based on the Cauchy-Born rule: “linear displacement of boundary implies linear displacements of molecular lattice”
- Original paper [Tadmor, Ortiz, Phillips, 1996]
- There exists Type A and Type B versions
- Representative atoms and P1 representation of continuum
- Variational formulation

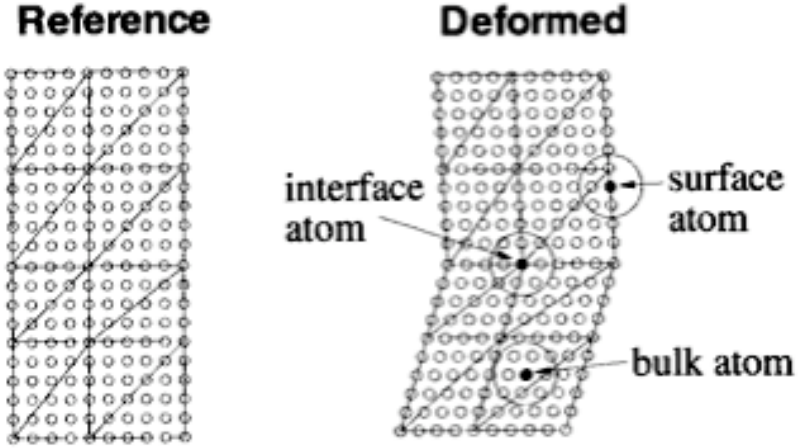
Reference
Deformed
interface atom
surface atom
bulk atom

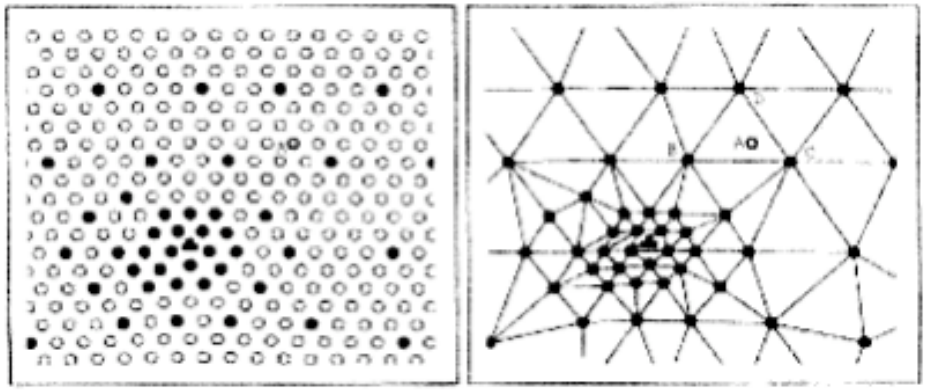

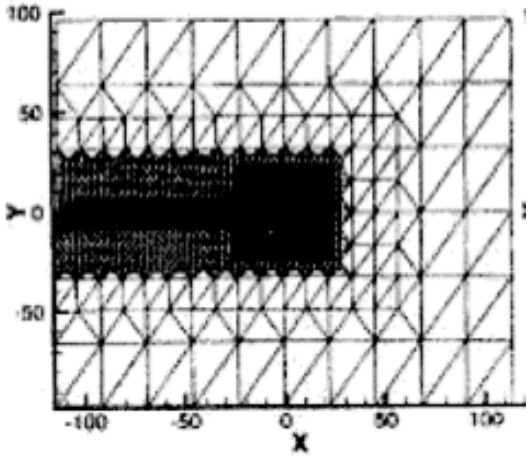
100
50
0
-50
Y
-100
-50
0
50
100
X

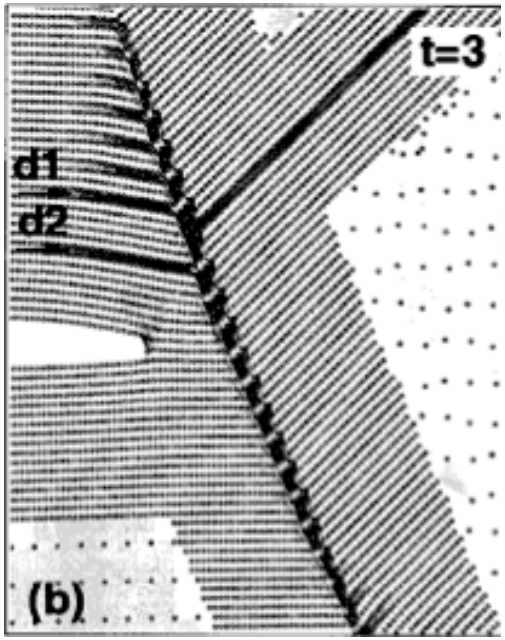
t=3
d1
d2
(b)

Ultra FFTs

- Complexity of computing B largest modes from N data points: O(BlogN) compare FFT: O(NlogN) and FT: $O(N^2)$
- Random algorithm: accuracy δ with probability 1 - ε
- For given frequency Fourier coefficient computed by MC

$$\frac{1}{M}\sum_m f_m e^{-i\omega x_m} \approx \int f(x) e^{-i\omega x} dx$$

- Frequency determined by hierarchical evaluation of L_2 norms of band limited filtered function values. Norm evaluation by MC
- [Gilbert and collaborators]

Equation free computations

- [Kevrekides and collaborators]
- General procedure: local simulations connected by extrapolations and interpolations
- Many successful applications

Gas kinetic schemes

- [Xu and collaborators]
- CFD fluxes computed by kinetic models at computational cell boundaries.

Superparametrization

- [NCAR]
- Turbulent vertical convection computed locally (reduced dimension) and used in global weather simulations

Example: a nonlinear conservation law is typically based on an empirical equation of state,

$$\rho_t + \nabla \cdot (v\rho) = 0$$
$$(\rho v)_t + \nabla \cdot (v\rho v + p) = 0$$
$$e_t + \nabla \cdot (ve + vp) = 0$$
$$p \approx (\gamma - 1)(e - \rho v^2/2)$$

The macro-scale fluxes may, for example,be computed on the fly by micro-scale kinetic Monte Carlo or molecular dynamics simulations,

$$m_j \frac{d^2 x_j(t)}{dt^2} = -\frac{\partial V_j(x)}{\partial x_j}, \quad j = 1, \ldots J$$

A generalized Godunov method: Set up approximation by a finite volume scheme for the effective nonlinear conservation law,

$$\frac{\partial u}{\partial t} + \frac{\partial}{\partial x} f(u) = 0, \qquad \bar{u}_j^n = \Delta x^{-1} \int_{x_{j-1/2}}^{x_{j+1/2}} u(\xi, t_n) d\xi$$

$$\bar{u}_j^{n+1} = \bar{u}_j^n - \Delta t^{-1} \int_{t_n}^{t_{n+1}} (f(u(x_{j+1/2}, \tau)) - f(u(x_{j-1/2}, \tau)) d\tau$$

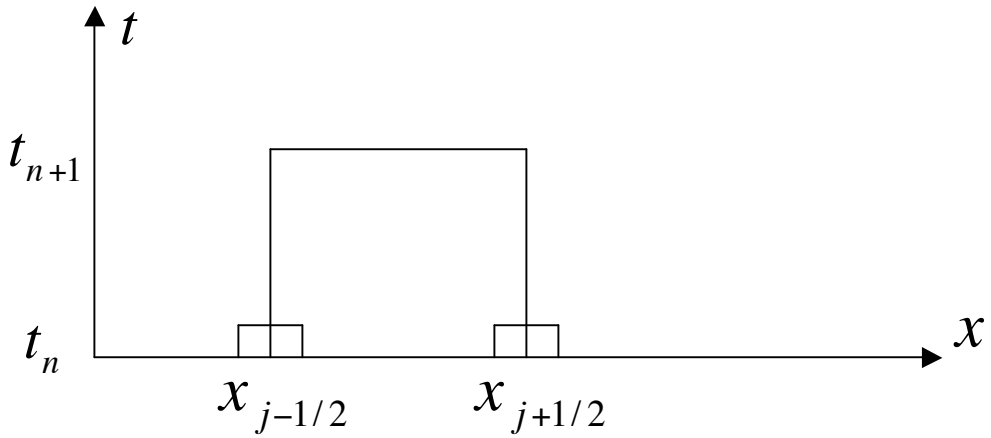

Estimate the flux *f* by replacing the Riemann solver in the Godunov scheme by a micro-scale simulation, with appropriate initial and boundary conditions.

A generalized Godunov method: Set up approximation by a finite volume scheme for the effective nonlinear conservation law,

$$\frac{\partial u}{\partial t} + \frac{\partial}{\partial x} f(u) = 0, \qquad \bar{u}_j^n = \Delta x^{-1} \int_{x_{j-1/2}}^{x_{j+1/2}} u(x, t_n)\, dx$$

$$\bar{u}_j^{n+1} = \bar{u}_j^n - \Delta t^{-1} \int_{t_n}^{t_{n+1}} (f(u(x_{j+1/2}, t)) - f(u(x_{j-1/2}, t)))\, dt$$

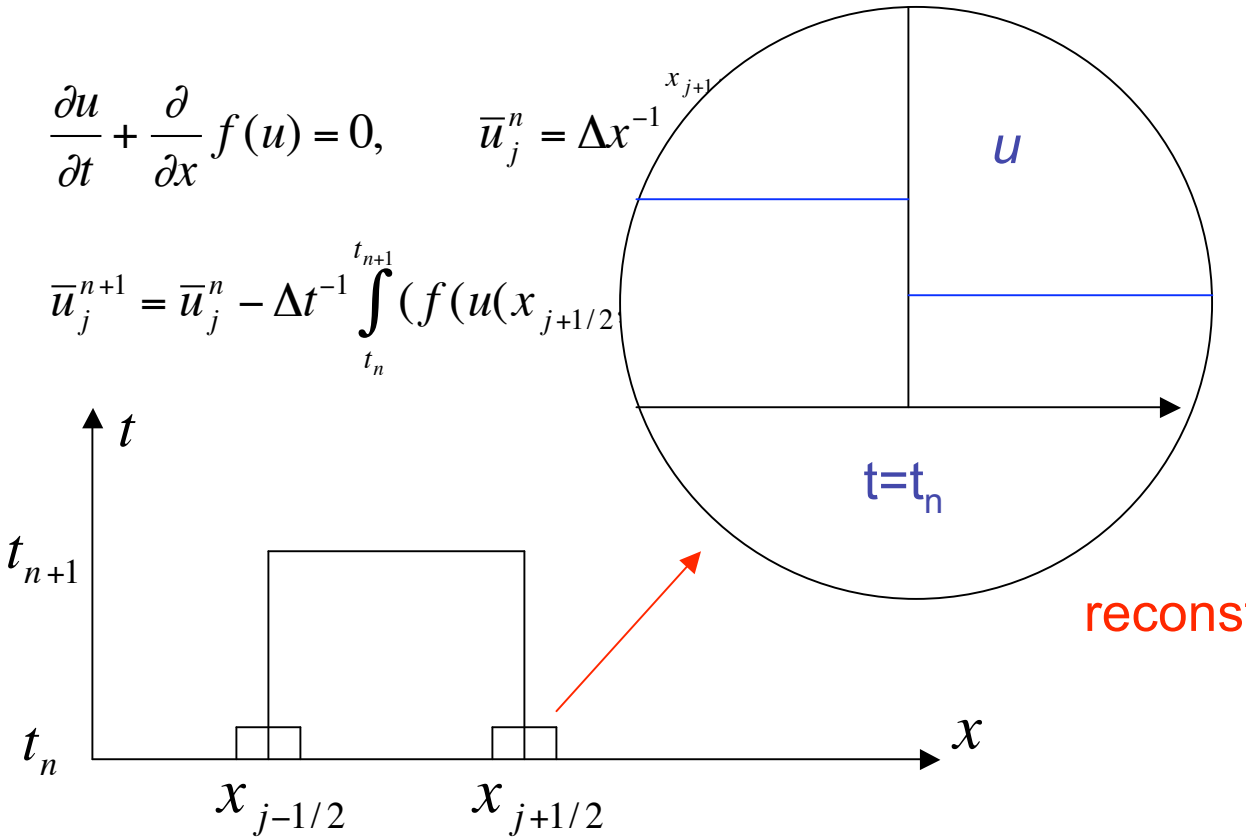

Estimate the flux *f* by replacing the Riemann solver in the Godunov scheme by a micro-scale simulation, with appropriate initial and boundary conditions.

A generalized Godunov method: Set up approximation by a finite volume scheme for the effective nonlinear conservation law,

$$\frac{\partial u}{\partial t} + \frac{\partial}{\partial x} f(u) = 0, \qquad \bar{u}_j^n = \Delta x^{-1} \int_{x_{j+1}}^{} (u(x$$

$$\bar{u}_j^{n+1} = \bar{u}_j^n - \Delta t^{-1} \int_{t_n}^{t_{n+1}} (f(u(x_{j+1/2}$$

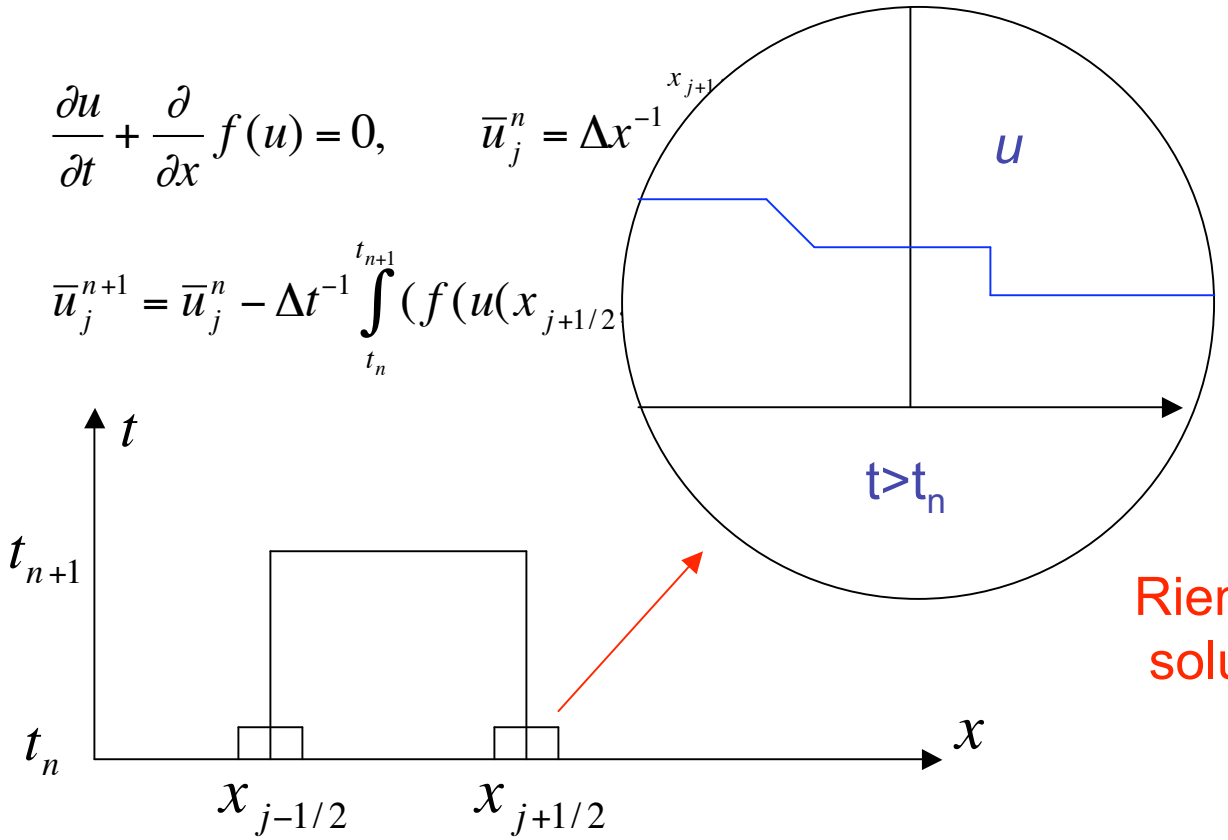

Riemann solution

Estimate the flux *f* by replacing the Riemann solver in the Godunov scheme by a micro-scale simulation, with appropriate initial and boundary conditions.

A generalized Godunov method: Set up approximation by a finite volume scheme for the effective nonlinear conservation law,

$$\frac{\partial u}{\partial t} + \frac{\partial}{\partial x} f(u) = 0, \qquad \bar{u}_j^n = \Delta x^{-1} \int_{x_{j-1/2}}^{x_{j+1/2}}$$

$$\bar{u}_j^{n+1} = \bar{u}_j^n - \Delta t^{-1} \int_{t_n}^{t_{n+1}} (f(u(x_{j+1/2}$$

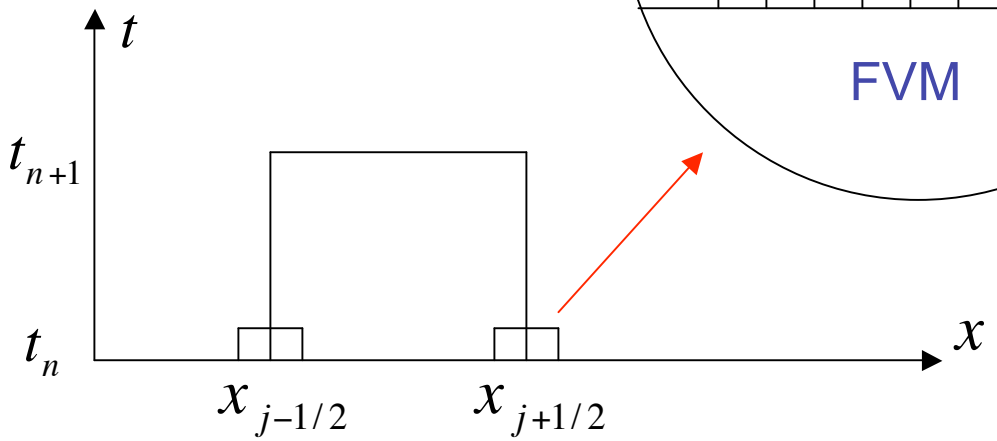

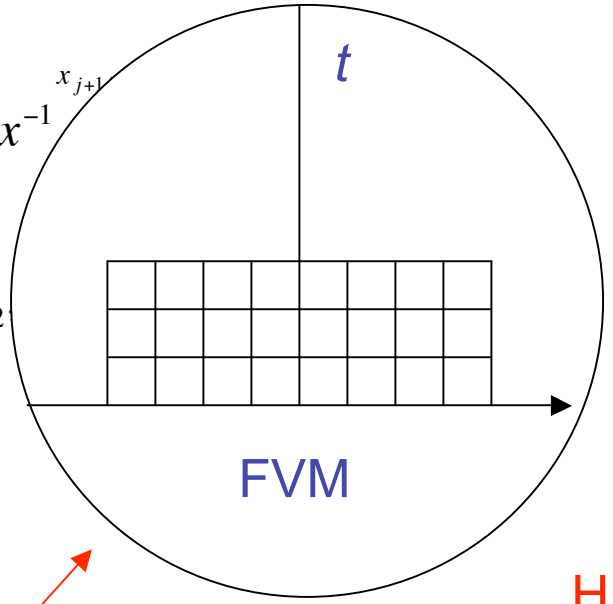

HMM

Estimate the flux *f* by replacing the Riemann solver in the Godunov scheme by a micro-scale simulation, with appropriate initial and boundary conditions.

A generalized Godunov method: Set up approximation by a finite volume scheme for the effective nonlinear conservation law,

$$\frac{\partial u}{\partial t} + \frac{\partial}{\partial x} f(u) = 0, \qquad \bar{u}_j^n = \Delta x^{-1} \int_{x_{j-1/2}}^{x_{j+1/2}}$$

$$\bar{u}_j^{n+1} = \bar{u}_j^n - \Delta t^{-1} \int_{t_n}^{t_{n+1}} (f(u(x_{j+1/2}$$

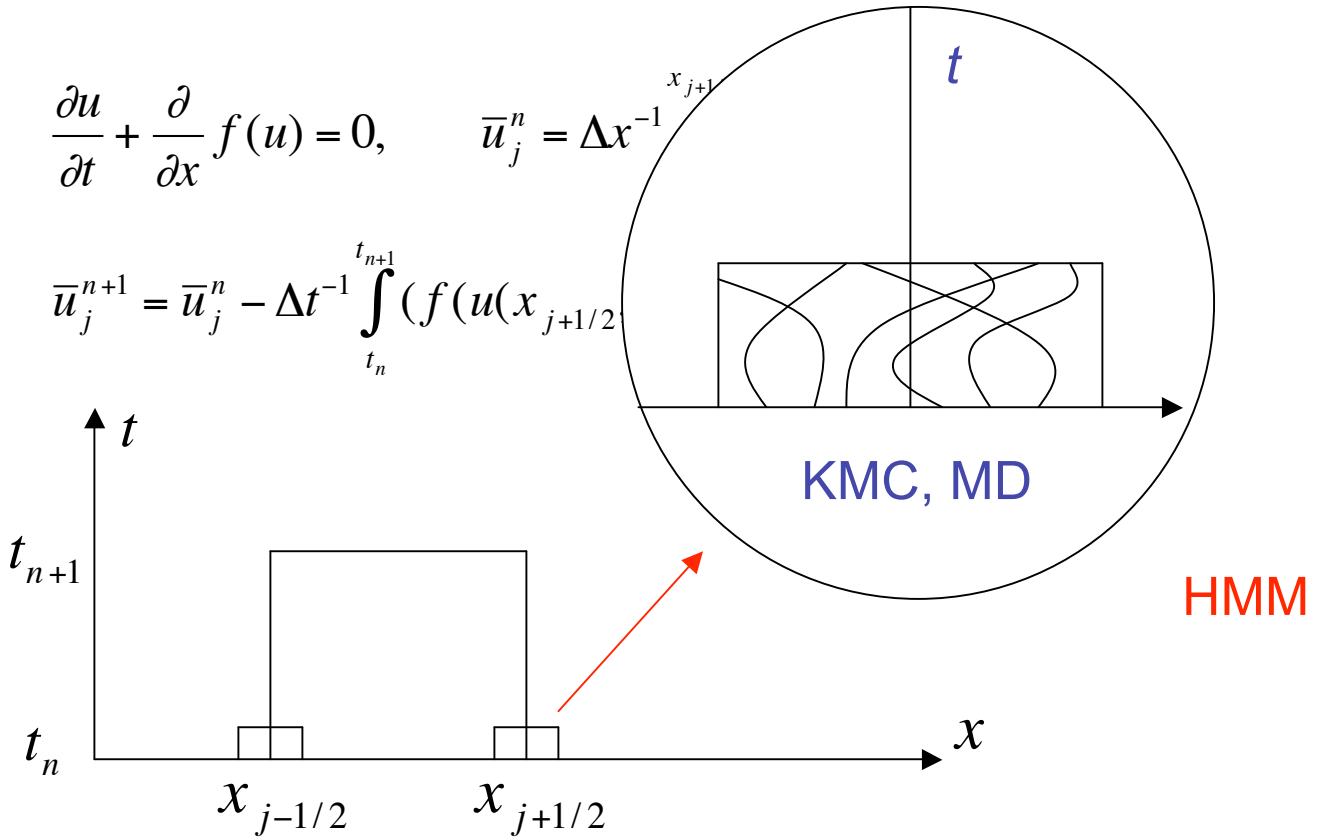

HMM

Estimate the flux *f* by replacing the Riemann solver in the Godunov scheme by a micro-scale simulation, with appropriate initial and boundary conditions.

A generalized Godunov method: Set up approximation by a finite volume scheme for the effective nonlinear conservation law,

$$\frac{\partial u}{\partial t} + \frac{\partial}{\partial x} f(u) = 0, \qquad \bar{u}_j^n = \Delta x^{-1} \int_{x_{j-1/2}}^{x_{j+1/2}} u(\xi, t_n) d\xi$$

$$\bar{u}_j^{n+1} = \bar{u}_j^n - \Delta t^{-1} \int_{t_n}^{t_{n+1}} (f(u(x_{j+1/2}, \tau)) - f(u(x_{j-1/2}, \tau)) d\tau$$

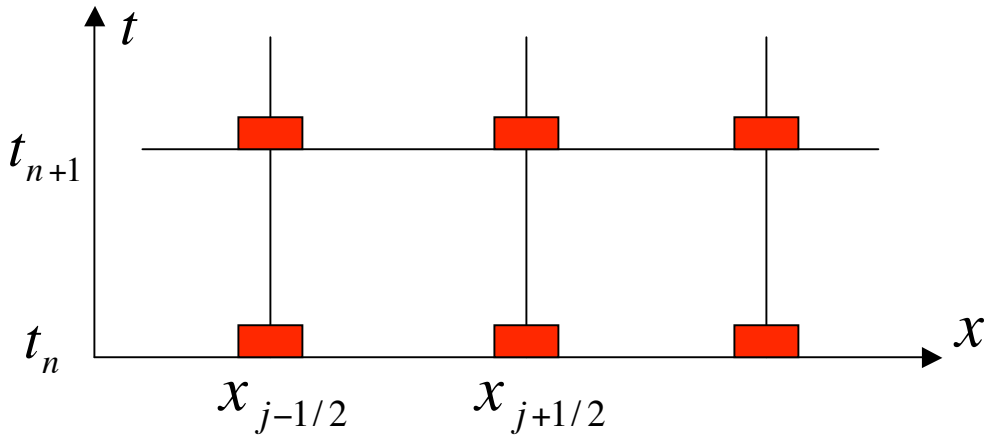

Efficiency follows from minimal use of micro-scale model (small L)

Carleman equations

Example of a different sampling strategy,

$$u_t + u_x = v^2 - u^2$$

$$v_t - v_x = u^2 - v^2$$

$$u(x,0) = u_0(x, x/\varepsilon), \quad v(x,0) = v_0(x, x/\varepsilon),$$

$$u(x,y), v(x.y) \quad 1-periodic\ in\ y$$

Homogenized equations, evolution of Young measure [Tartar]

$$U_t + U_x = \int_0^1 V(x,y)^2 dy - U^2$$

$$V_t - V_x = \int_0^1 U(x,y)^2 dy - V^2$$

$$U(x,y,0) = u_0(x,y), \quad V(x,y,0) = v_0(x,y)$$

It is possible to prove weak convergence for particle methods even when ε<h. Finite difference or finite element methods with phase or dissipative errors do not converge.

Proof based on small devisors argument. Compare convergence of quasi Monte Carlo methods. For given smooth test function we have

$$\lim_{h\to 0}(\sup^{*}_{0<\varepsilon\le\bar{\varepsilon}}(\sum_{j}((u_h^{\varepsilon})_j - u^{\varepsilon}(x_j))\varphi(x_j) = 0$$

$$\sup^{*} : for\ aa\ \varepsilon/h$$

6. Analysis - convergence results

- FVM for hyperbolic and parabolic equations and FEM for elliptic equations when applied to standard linear homogenization problems.
- FVM approximating the diffusion equation as by Brownian motion.
- FDM for selected dynamical systems and stochastic differential equations. Both dissipative and oscillatory problems.
- Typical error estimate (p order of macro-scale method), $e(HMM)$ error in data from micro-scale model

$$\left\| U_0 - U_{HMM} \right\| \leq C(H^p + e(HMM)),$$

Structure of analysis

$$Macro: \quad F_H(U_H, D_H(u_h)) = 0$$
$$Micro: \quad f_h(u_h, d_h(U_H)) = 0$$
$$\rightarrow \quad F_H(U_H, \tilde{D}_H(U_H)) = 0,$$

$$effective\ eqs: \quad \overline{F}(\overline{U}, \overline{D}(\overline{U})) = 0,$$
$$F_H(\overline{U}_H, \overline{D}_H(\overline{U}_H)) = 0, \quad (1)$$

$$Stability\ of\ (1): \quad \left\| U - U_H \right\| \le C(H^p + e(HMM))$$
$$e(HMM) = \left\| \overline{D} - \tilde{D} \right\|, \quad U_H \in W$$

Compare Strang's proof for convergence of FDM approximating nonlinear hyperbolic PDEs

Example: homogenization of elliptic equation

$$-\nabla \cdot (a^{\varepsilon}(x)\nabla u^{\varepsilon}(x)) = f(x), \quad x \in D \subset R^{d}$$

$$u^{\varepsilon}(x) = 0, \quad x \in \partial D, \quad a_1 \geq a^{\varepsilon} \geq a_0 > 0$$

Assume there exists a homogenized equation (not known)

$$-\nabla \cdot (A(x)\nabla U(x)) = f(x), \quad x \in D \subset R^{d}$$

$$U(x) = 0, \quad x \in \partial D, \quad A \geq A > 0$$

$$u^{\varepsilon} \to U, \quad \varepsilon \to 0$$

Ideally we want a FEM for the homogenized equation based on the bilinear form

$$A(V,W) = \int_D \nabla V(x) \cdot A(x) \nabla W(x) dx$$

$$\min_{V_H \in \boldsymbol{V_H}} \left(\frac{1}{2} A(V_H, V_H) - (f, V_H)\right)$$

where $\boldsymbol{V_H}$ is a standard finite element space (ie. P_1, Dirichlet bc.). With T_H the corresponding triangulation of D we have the numerical approximation

$$A(V_H, V_H) \approx A_H(V_H, V_H) = \sum_{K \in T_H} |K| \sum_{x_l \in K} \omega_l (\nabla V_H \cdot A(x) \nabla V_H)(x_l)$$

The HMM strategy is now to approximate the unknown stiffness matrix (A(x) is not known) by constrained micro-scale simulations

$$(\nabla V_H \cdot A \nabla V_H)(x_l) \approx \frac{1}{\delta^d} \int_{I_\delta(x_l)} \nabla v_l^\varepsilon(x) \cdot a^\varepsilon(x) \nabla v_l^\varepsilon(x) dx$$

Where $I_\delta(x_l)$ is a cube with side length δ centered at x_l. Boundary conditions for micro-scale problem to mach gradient of V_H via Dirichlet, Neumann or periodic conditions.

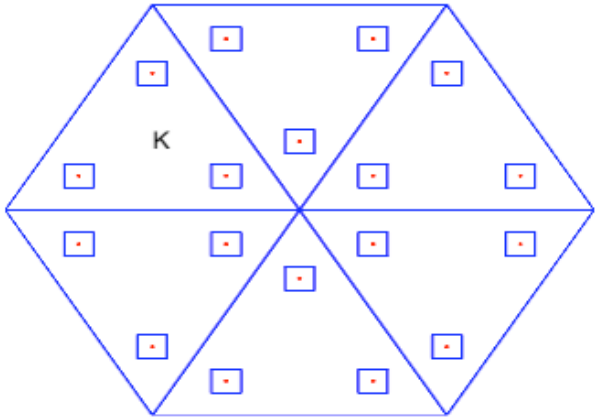

An alternative way for the same formulation

$$\min_{v_h \in \boldsymbol{v_h}} (a(v_h, v_h) - 2(f, v_h)) =$$

$$= \min_{V_H \in \boldsymbol{V_H}} \left(\min_{v_h \in \boldsymbol{v_h} \setminus V_H} (a(v_h, v_h) - 2(f, v_h)) \approx \min_{V_H \in \boldsymbol{V_H}} (\tilde{A}(V_H, V_H) - 2(f, V_H)) \right.$$

The validity of the last step that includes the quadrature is based on localization and scale separation.

In a Galerkin formulation the following inner product are computed

$$(\nabla \Phi_j \cdot A \nabla \Phi_k)(x_l) \approx \frac{1}{\delta^d} \int_{I_\delta(x_l)} \nabla v_l^\varepsilon(x) \cdot a^\varepsilon(x) \nabla w_l^\varepsilon(x) dx$$

where boundary conditions for v and w match $\nabla\Phi$.

Convergence results for the elliptic homogenization case with

$$a^{\varepsilon}(x) = a(x, x/\varepsilon), \quad a(x,y),\ regular\ and\ 1-periodic\ in\ y$$
$$a(x,\omega),\ random\ stat.inv.under\ 1-shifts$$

Let U_0 be the analytical homogenized solution and U_{HMM} the computed HMM-solution. Assume the macro scheme uses P_k elements and that the quadrature formulas are exact for polynomials of order 2k-2. Define

$$e(HMM) = \max_{\substack{x_l \in K \\ K \in T_H}} \left| A(x_l) - A_H(x_l) \right|$$

Theorem, Let h→0, $a = a(x, x/\varepsilon)$

$$\left\| U_0 - U_{HMM} \right\|_s \le C(H^{p+1-s} + e(HMM)), \quad s = 1,2$$

$$e(HMM) = \max_{\substack{x_l \in K \\ K \in T_H}} \left| A(x_l) - A_H(x_l) \right|$$

$$e(HMM) \le C((h/\delta)^q) \quad if\ \delta\ is\ multiple\ of\ \varepsilon, periodic$$

$$e(HMM) \le C(\varepsilon/\delta + \delta) \quad else, periodic, \quad (h \to 0)$$

$$e(HMM) \le C(\varepsilon/\delta)^{1/2}, \quad 1-D, random, \quad (h \to 0)$$

$$e(HMM) \le C(\varepsilon/\delta)^{0.23}, \quad 3-D, random, \quad (h \to 0)$$

The proof is based on the explicit form of the analytic solution [Abdul, Schwab], [E, Ming, Zhang]

$$u^\varepsilon(x) = U_0(x) + \varepsilon U_1(x, x/\varepsilon) + \varepsilon^2 U_2(x, x/\varepsilon) + .. + \varepsilon U_B^\varepsilon(x)$$

7. Examples of HMM simulations

- Fluid simulations: [E, Ren], contact line on multiphase fluid solid interaction. Type A example: Continuum model valid but for contact line where MD is applied.
- Solid simulation: [E, Li], thermal expansion.Type B example: Micro-scale finite temperature MD model needed in full domain of elasticity continuum model.
- Combustion fronts: [Sun, Eq], micro-scale simulation with chemistry to evaluate macro scale properties at front.
- Stiff dynamical systems: [Sharp, Eq, Tsai]. intervals with short time steps to evaluate the effective force for macro time steps.
- Epitaxial growth: [Sun, Eq], atomistic kinetic Monte Carlo micro-scale simulation - diffusion and level-set models for macro-scale.

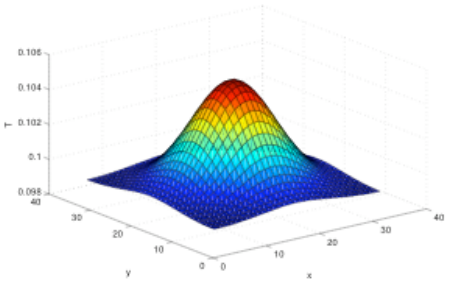

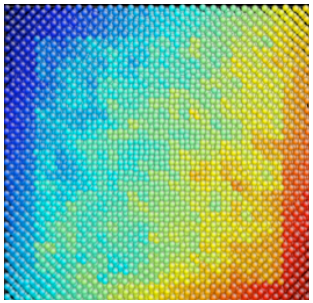

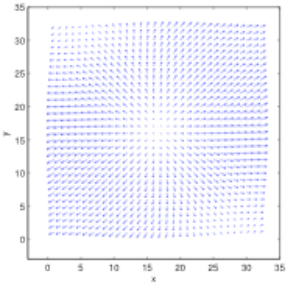

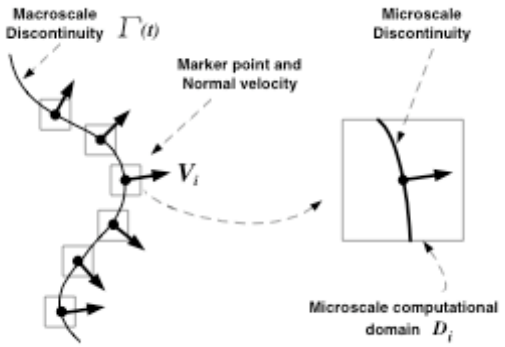
Macroscale
Discontinuity
$\Gamma(t)$
Marker point and
Normal velocity
V_i
Microscale
Discontinuity
Microscale computational
domain D_i

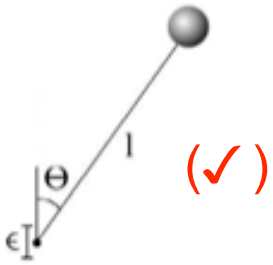
l
Θ

(✓)

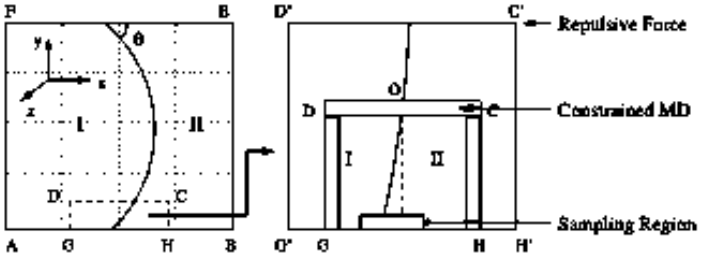
F
B
θ
y
x
I
II
D
C
A
G
H
B
D'
C'
O
D
C
I
II
O'
G
H
H'
Repulsive Force
Constrained MD
Sampling Region

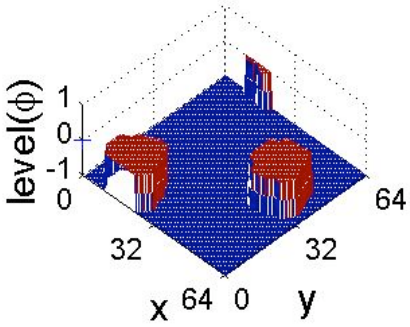
level(ϕ)
1
0
-1
0
32
64
32
x
64
0
y

(✓)

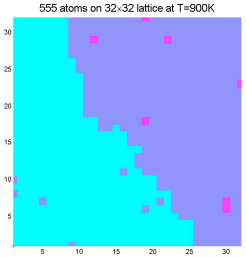
555 atoms on 32×32 lattice at T=900K

7.1 Multi-scale dynamical systems

- Examples: stiff dynamical systems and equations with rapidly changing coefficients
- Stiff systems

$$\frac{dx_\varepsilon}{dt} = f_\varepsilon(x_\varepsilon), \quad t > 0, \quad x_\varepsilon : R \to R^d$$

$$x_\varepsilon(0) = x_0, \quad \left\| \frac{\partial f_\varepsilon}{\partial x_\varepsilon} \right\| >> 1$$

The Kapitza pendulum, modeled by an equation with rapidly changing coefficient

$$l\frac{d^2\theta}{dt^2} = (g + \varepsilon^{-1}\sin(2\pi\varepsilon^{-1}t))\sin(\theta)$$

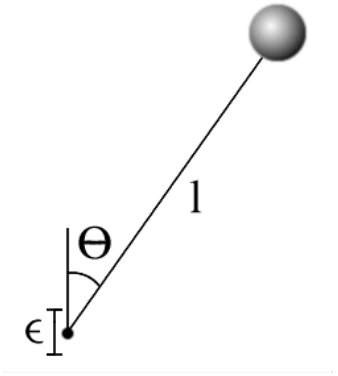

If the pivot is forced to oscillate rapidly, slow stable oscillations around θ =0 are possible.

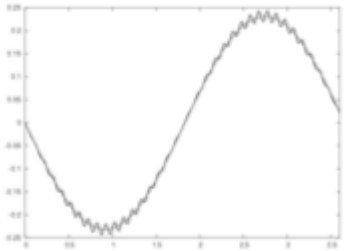

Structure of HMM-algorithm for ODEs

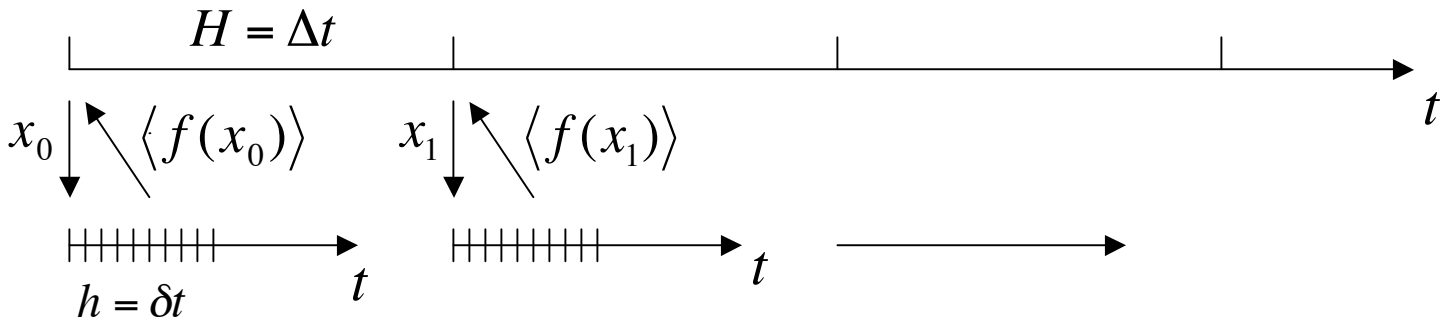

- Initiate micro-scale solver from the available macro-scale variables (micro-scale states or averages): reconstruction

- Effective $\langle f \rangle$ value for standard macro-scale solver from average of standard micro-scale data

Example: sun-earth-moon, Newton's equations

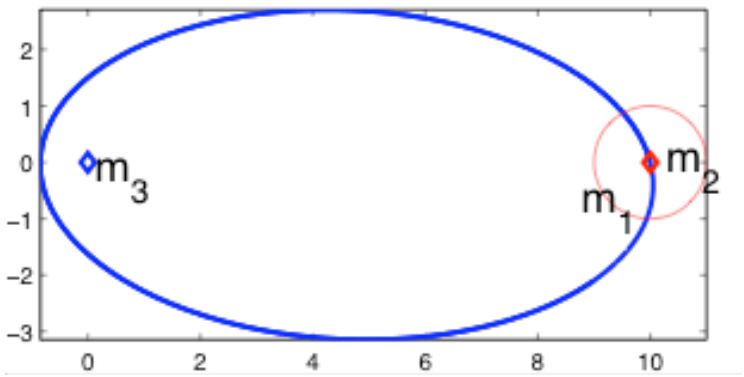

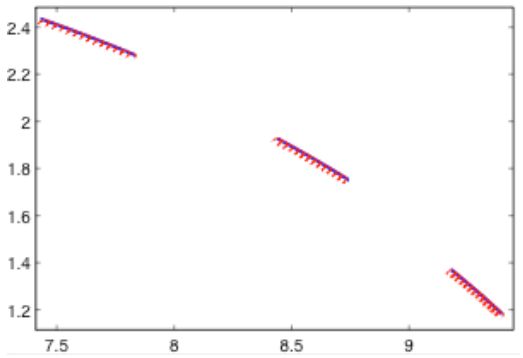

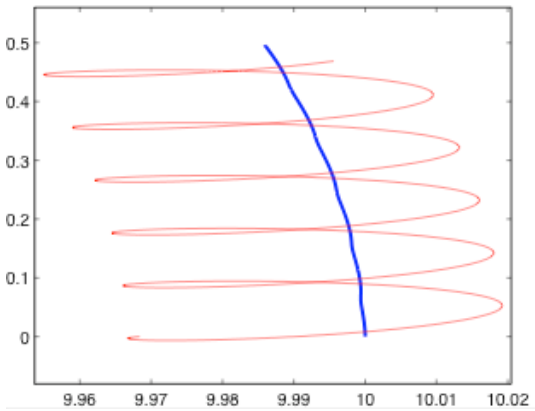

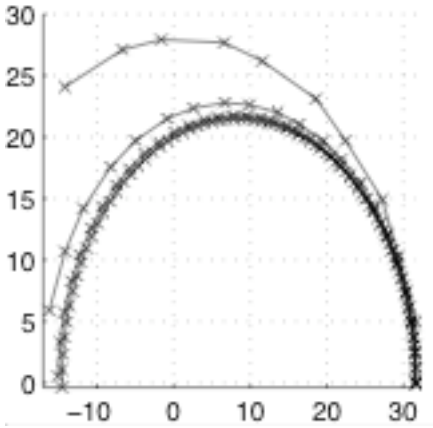

Remarks

- Averages approximate the following expression

$$\left\langle y^{\varepsilon}(t)\right\rangle = \lim_{\delta\to 0}(\lim_{\varepsilon\to 0}(\,\delta^{-1}\int_{t-\delta/2}^{t+\delta/2} y^{\varepsilon}(\tau)d\tau))$$

by $$\left\langle y_j\right\rangle = h\sum_k K(y_j - y_k)y_k$$

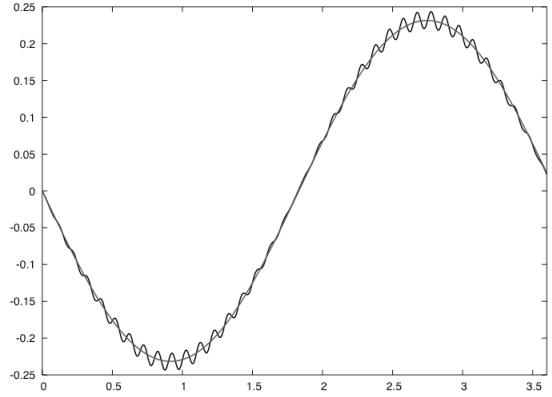

- *K* should satisfy regularity, support and moment conditions

$$K \in C^q; \quad K \equiv 0,\ y \notin (\tilde{y}, \tilde{y}+\eta);$$

$$\int (K(y) - \delta(y))y^r dy = 0,\ r = 0,..,R$$

The standard ODE-HMM for which macro and micro-scale variables are the same converges for linear problems with the appropriate order of accuracy if based on

- Stable and p-th order macro algorithm
- Stable and consistent micro algorithm
- Continuous averaging kernel with positive number of matched moments

$$\lim_{\eta \to 0}(\lim_{\varepsilon \to 0}(\lim_{h \to 0}\left\| \left\langle x(t_j) \right\rangle - \left\langle x_j \right\rangle \right\|)) \le CH^p$$

- Reconstruction and compression are identity maps
- The efficiency depends on kernel regularity and moment matching and on the order of micro-scale algorithm.

Example : the Kapitza pendulum

$$l\frac{d^2\theta}{dt^2} = (g + \varepsilon^{-1}\sin(2\pi\varepsilon^{-1}t))\sin(\theta)$$

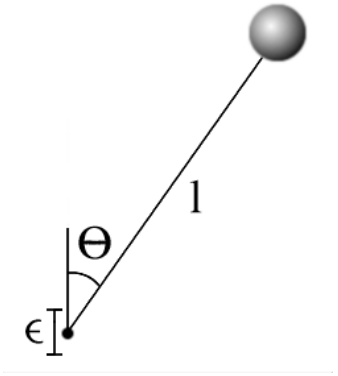

Phase matching is important.
Resonance can be controlled by adding $\langle\theta\rangle$ as variable.

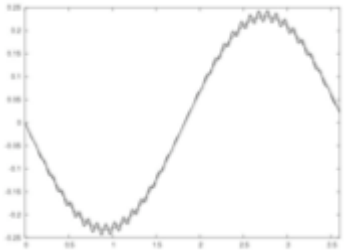

Convergence

The micro-scale variables are required to match $\langle \theta \rangle$.

Convergence proof following the general HMM outline. The error e(HMM) is estimated based on an averaging theorem, [Levi]. Second order convergence in *H* for the mid point rule applied to both micro and macro scales.

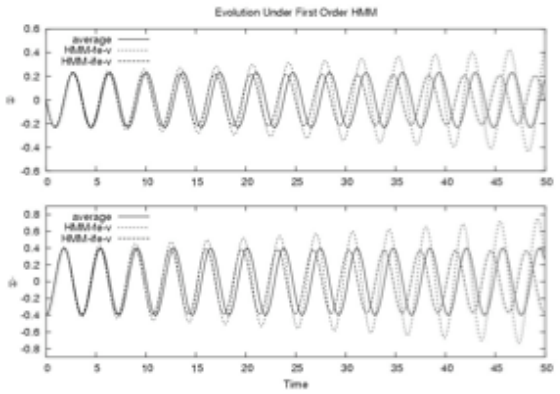

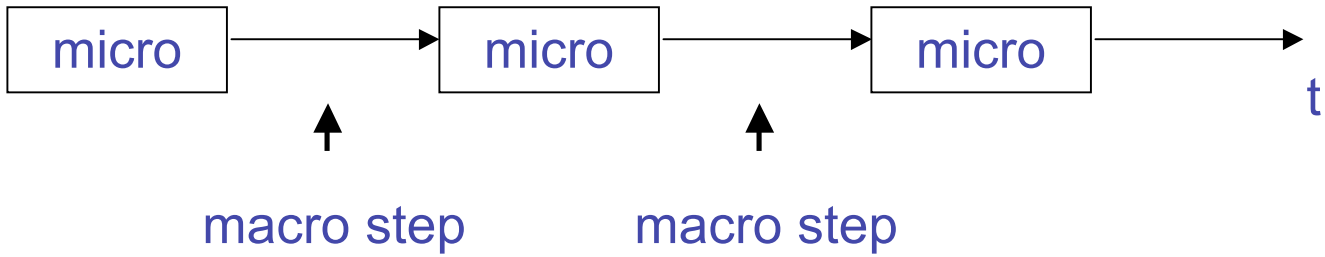
micro
micro
micro
t
macro step
macro step

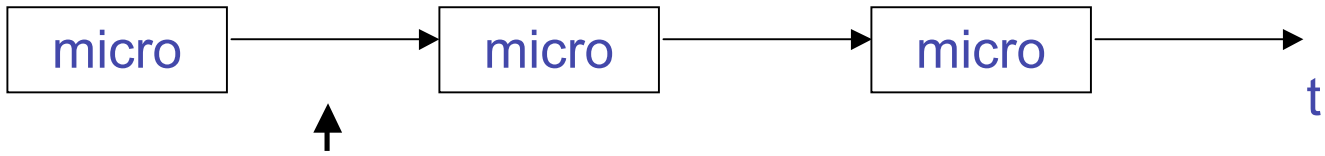

macro step

loss of information

resonance, phase

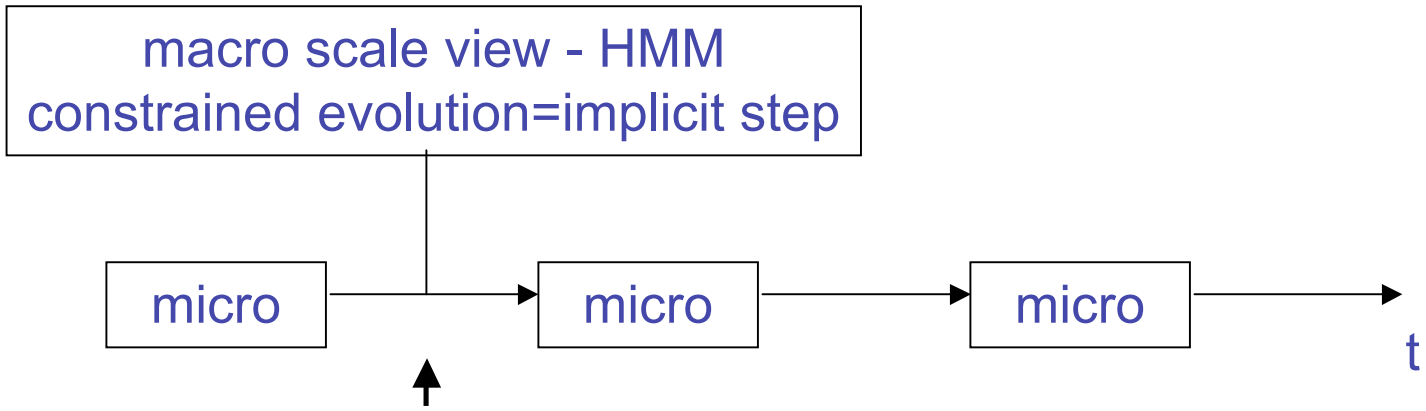

loss of information

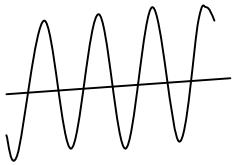

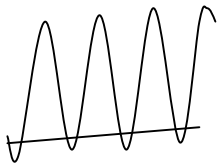

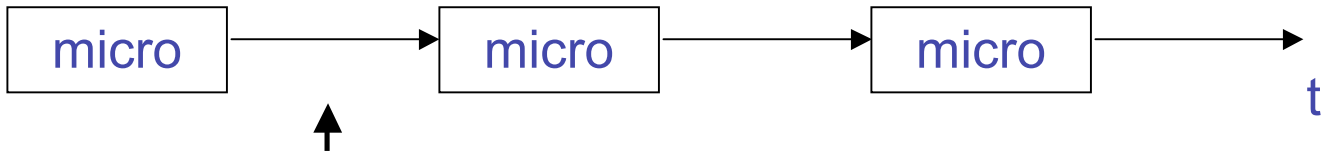

macro step

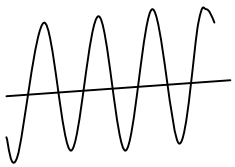

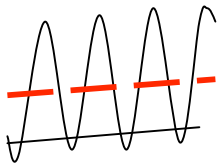

Unconstrained reconstruction misses the average

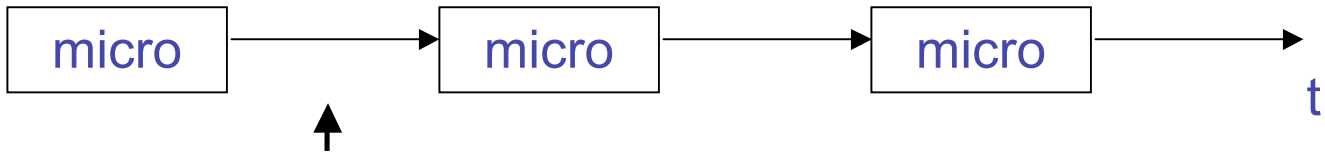

macro step

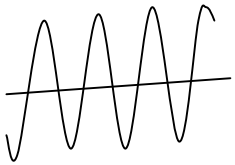

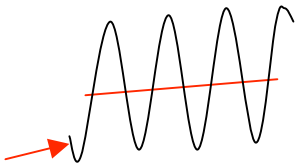

Implicit reconstruction to match predicted $\langle \theta \rangle$ based on Newton step as in stiff ODE solvers. Compare thermostats in MD

With a different resonance scenario extra macro-scale variables may be required. Consider the stiff nonlinear system,

$$\frac{dx_1}{dt} = \varepsilon^{-1} x_2 + x_1, \qquad x_1(0) = 0$$

$$\frac{dx_2}{dt} = -\varepsilon^{-1} x_1 + x_2, \qquad x_2(0) = 1$$

$$\frac{dx_3}{dt} = x_1^2, \quad x_3(0) = 0$$

$$\rightarrow x_1 = e^t \sin(\varepsilon^{-1} t), \quad x_2 = e^t \cos(\varepsilon^{-1} t),$$

$$x_3 = (e^{2t} - 1)/2$$

By also tracking $\langle (x_1)^2 \rangle$ and reinitialize such that the moment average is consistent, convergence can be achieved. Emerging theory based on normal form.

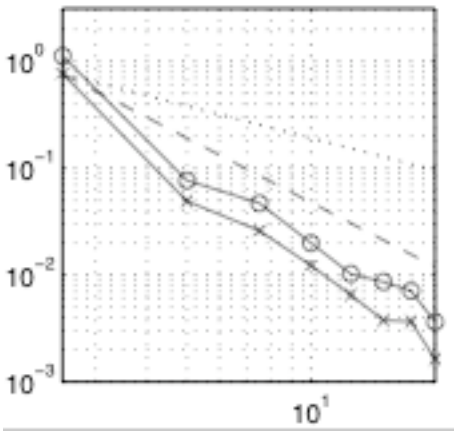

7.2 . Epitaxial growth

- Part of semiconductor production
- Layer by layer deposition of atoms
- Atoms diffuse on substrate surface, merge and nucleate islands

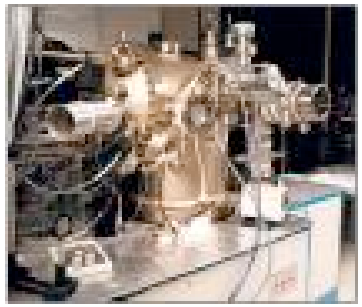

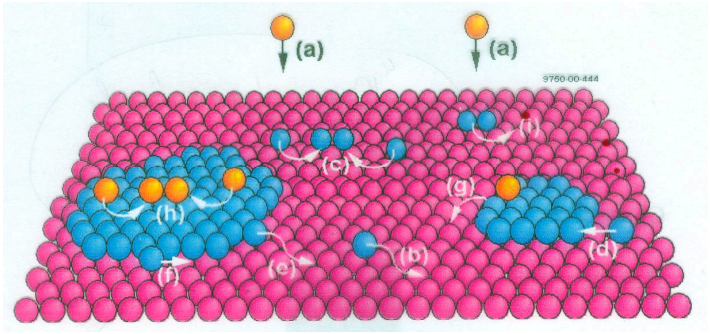

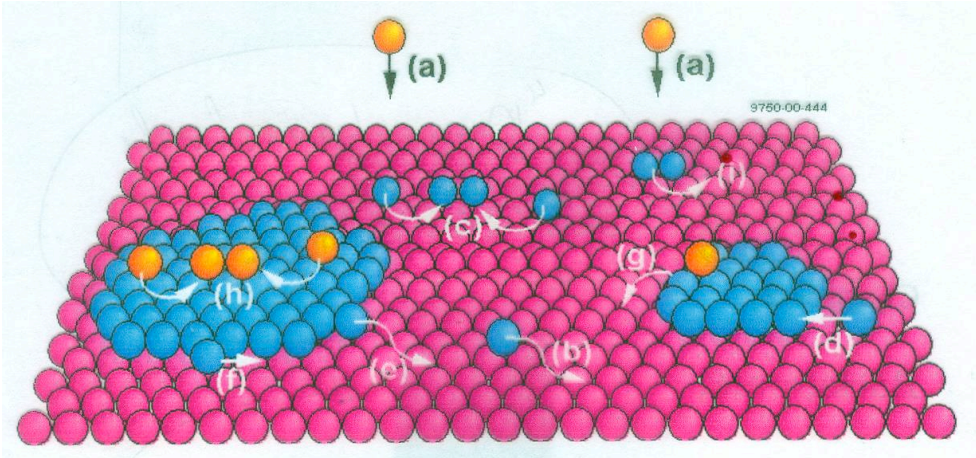

(a) Deposition (b) Diffusion (c) Nucleation (d) Attachment
(e) Detachment (f) Edge diffusion (g) Down step diffusion
(h) Nucleation on top of islands (i) Dimer diffusion

HMM strategy

- Macro-scale model: finite difference approximation of diffusion equation (ρ) coupled to level-set method for interface tracking (Γ).
- Missing data: velocity model for interface evolution and boundary conditions at interface.
- Micro-scale model: Kinetic Monte Carlo simulation of atom dynamics. Potentially based on density function computations of transition probabilities.

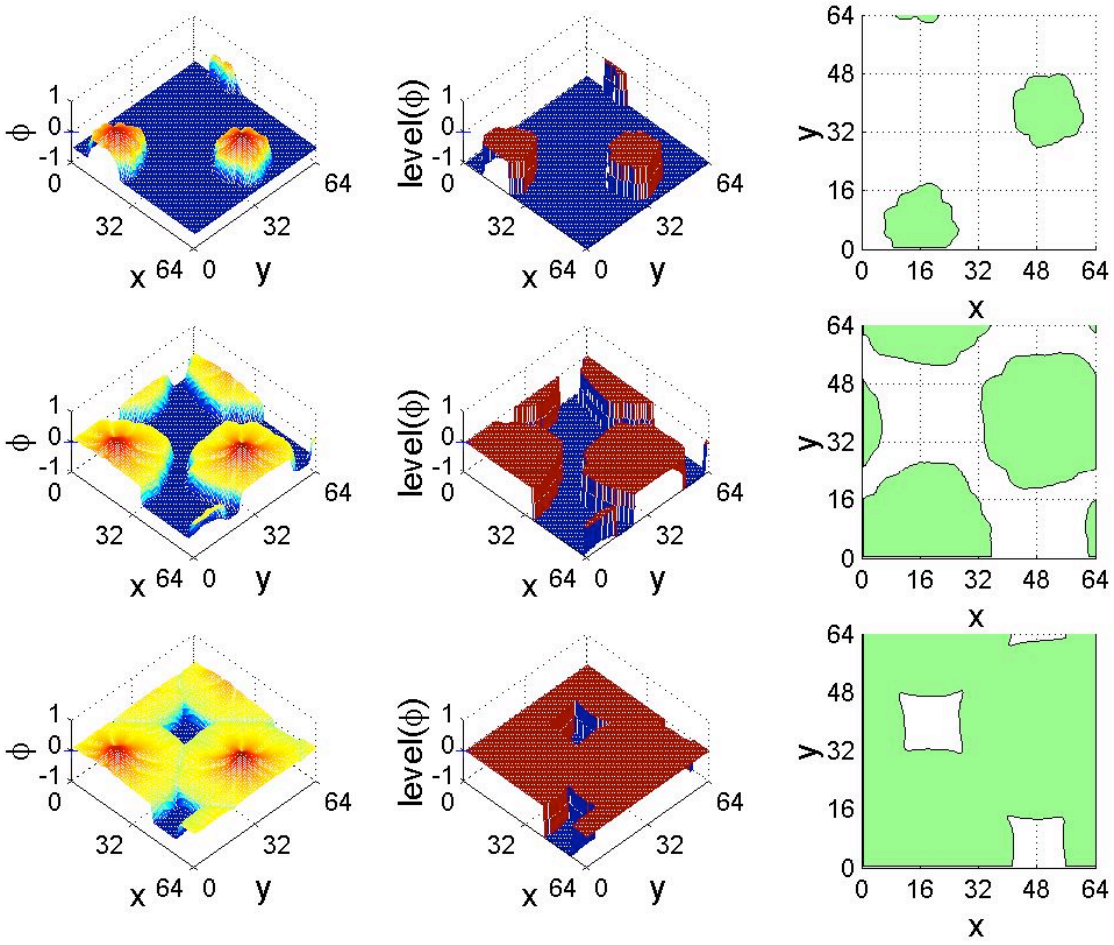

Masro-scale: diffusion equation and levelset
Interface tracking

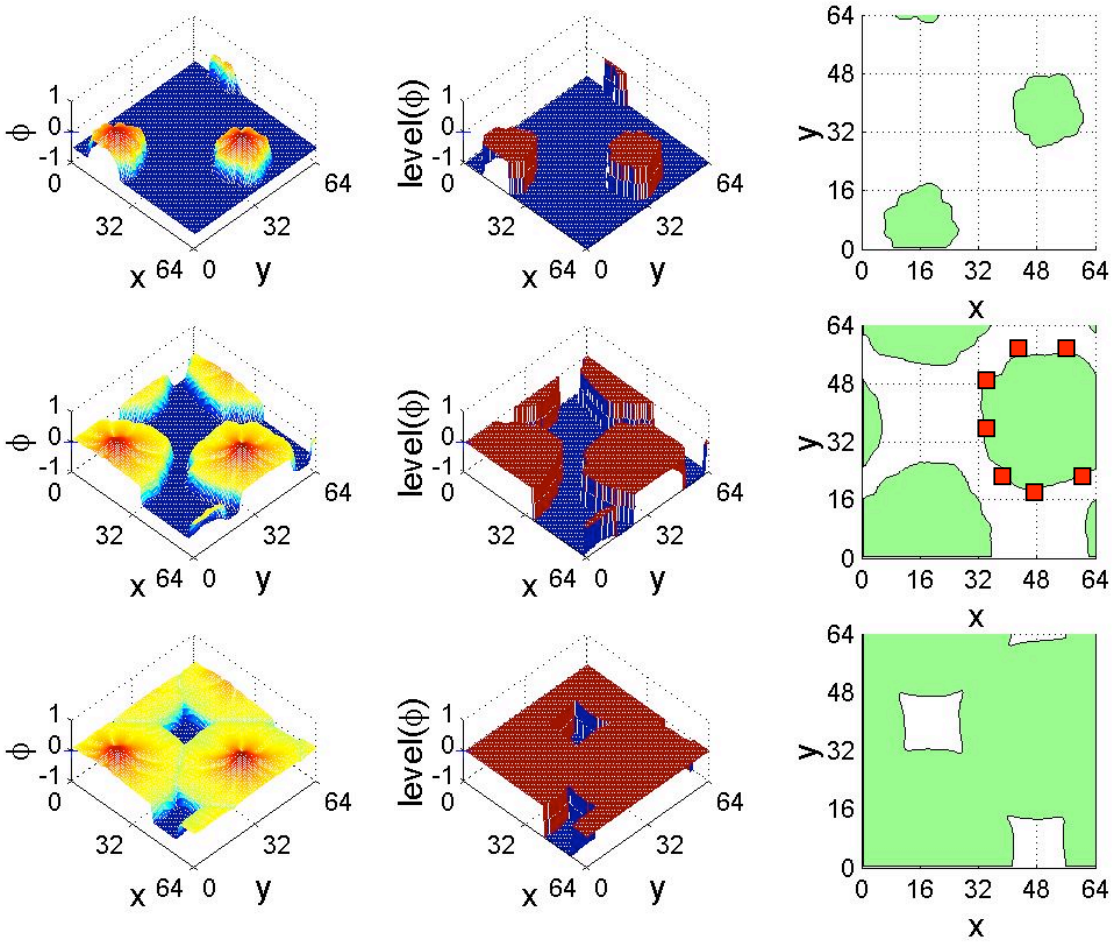

Masro-scale: diffusion equation and levelset
Interface tracking - Typa A and B

Micro-scale: atomistic Kinetic Monte Carlo, Initial and boundary conditions from macro-scale, returning front velocity and front boundary conditions.

Roughness of interface important for front velocity

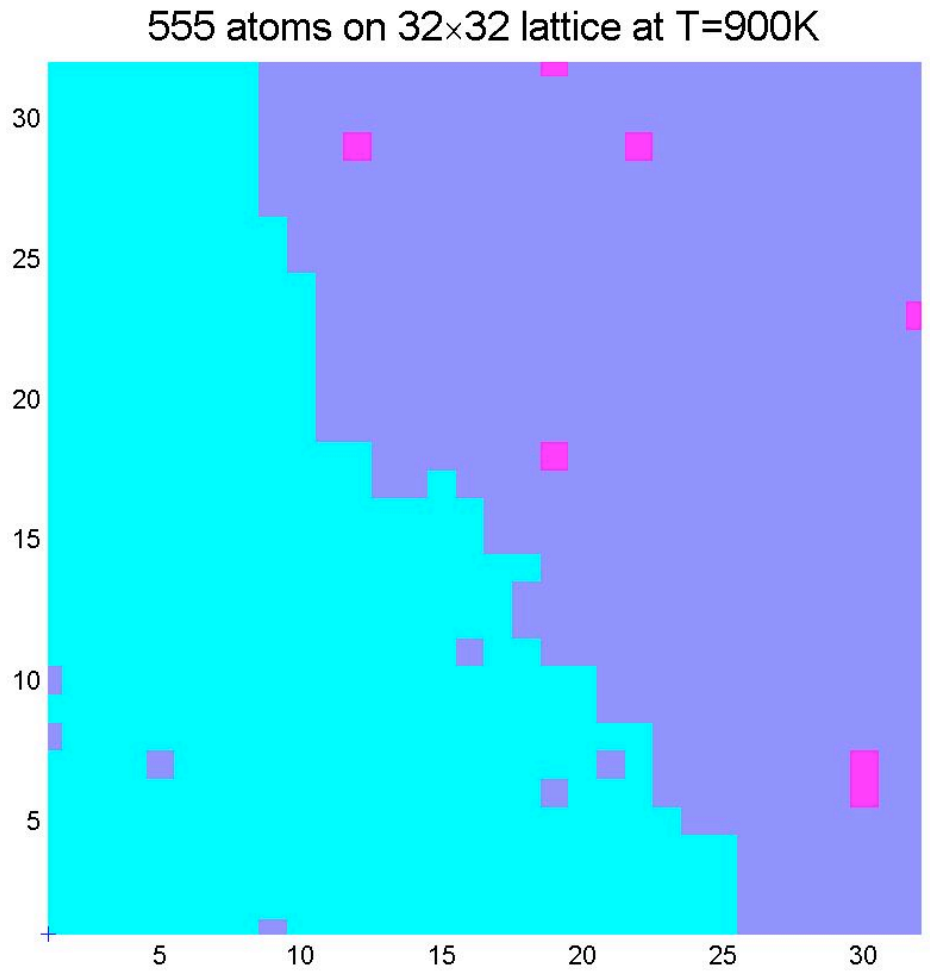

Outline of algorithm

1. Macro-scale step
   - 1.1 Update the level-set function representing Γ based on velocity estimate from earlier micro-step
   - 1.2 Update ρ by implicit finite differences and the preconditioned conjugate gradient method using new location of Γ and Robin boundary condition from micro-step

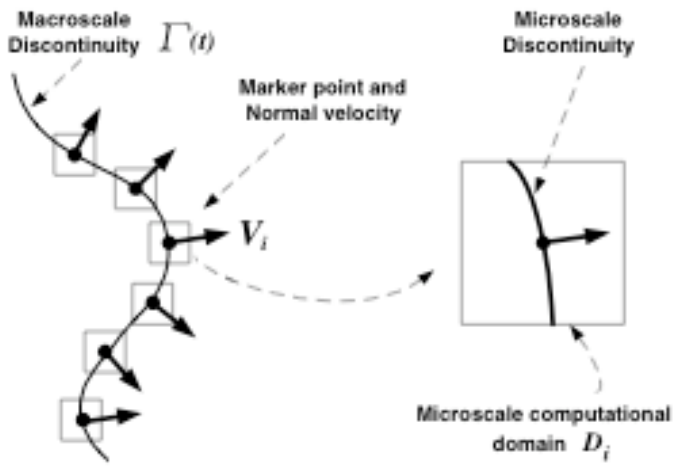

2. Micro-scale step
   - 2.1 Generate initial distribution of atoms using results from step 1
   - 2.2 Perform a number of Kinetic Monte Carlo steps based on empirical or pre-computed probabilities
   - 2.3 Outer boundary conditions for flux balance given ρ from 1.2
   - 2.4 Estimate velocity of Γ and flux boundary conditions for 1.1 and 1.2

8. Computational issues

- New techniques
- Concurrent or sequential?
- Need for scale separation?
- Top down or bottom up?
- Choice of macro-scale variables

8.1 New techniques

- Reconstruction techniques (from macro states to micro data)
- Boundary conditions for local micro-scale simulations
- Data estimation (from micro data to macro model)

- These techniques are also needed when when a refined simulation is used to derive fixed effective equations

New techniques - the conservation law problem

- Reconstruction techniques (from macro states to micro data)
- Boundary conditions for local micro-scale simulations
- Data estimation (from micro data to macro model)

- These techniques are also needed when when a refined simulation is used to derive fixed effective equation

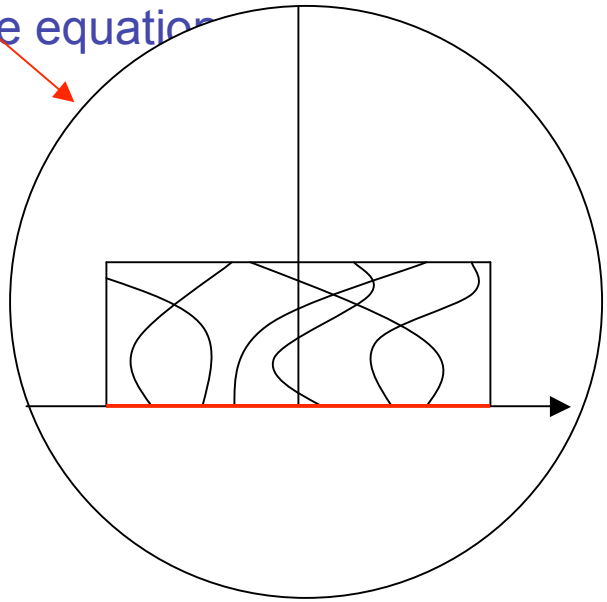

New techniques - the conservation law problem

- Reconstruction techniques (from macro states to micro data)
- Boundary conditions for local micro-scale simulations
- Data estimation (from micro data to macro model)

- These techniques are also needed when when a refined simulation is used to derive fixed effective equation

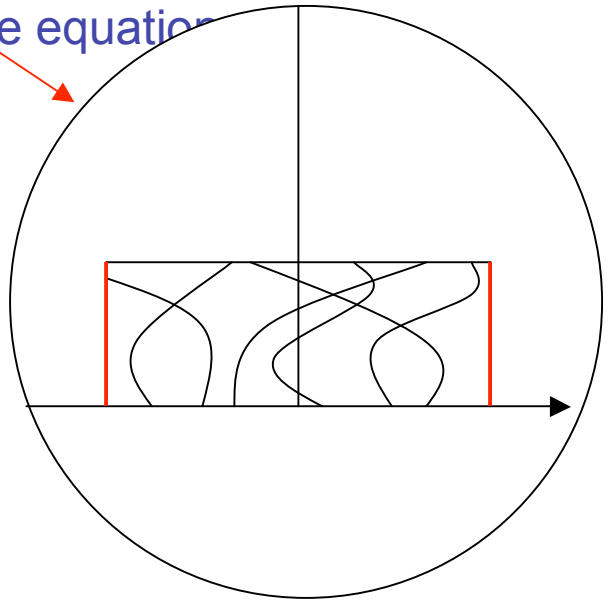

New techniques - the conservation law problem

- Reconstruction techniques (from macro states to micro data)
- Boundary conditions for local micro-scale simulations
- Data estimation (from micro data to macro model)

- These techniques are also needed when when a refined simulation is used to derive fixed effective equation

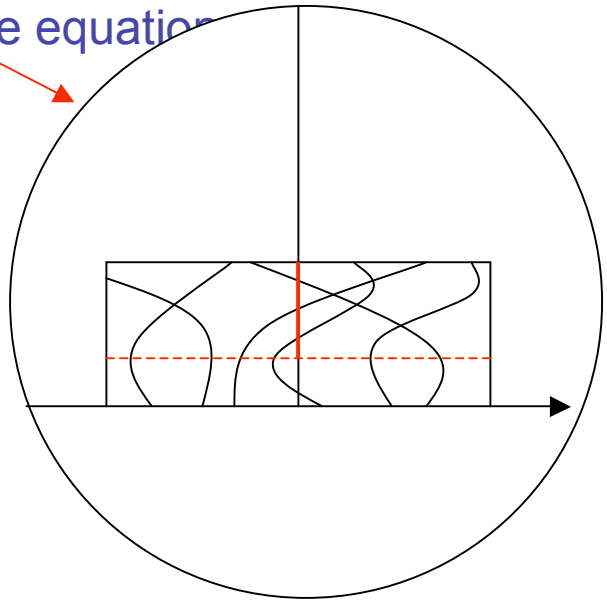

8.2 Concurrent or sequential?

- In sequential simulations, the micro-scale computations produce tables for the unknown data ahead of the macro-scale simulation
- Also called parameter passing or pre-computing
- As described HMM is concurrent. The macro- and micro-scales are coupled throughout the simulation
- The choice is a matter of computational cost

Example: the calculation of atomistic transition probabilities in the epitaxial growth application can be tabulated as a finite number of functions of temperature. More efficient that concurrent computations in two dimensional space-time.

Example: in the epitaxial growth computations the velocity depends on density above and below the step as well as on temperature and orientation of step versus the crystal lattice. The sequential method requires exploration of a four dimensional space instead of the two dimensional x-t space for concurrent simulation.

8.3 Need for scale separation?

- HMM for type B problems requires substantial scale separation to be efficient
- Compare techniques as, for example, multi-grid for which scale separation not essential
- HMM for type A problems does not require scale separation

8.4 Top down or bottom up

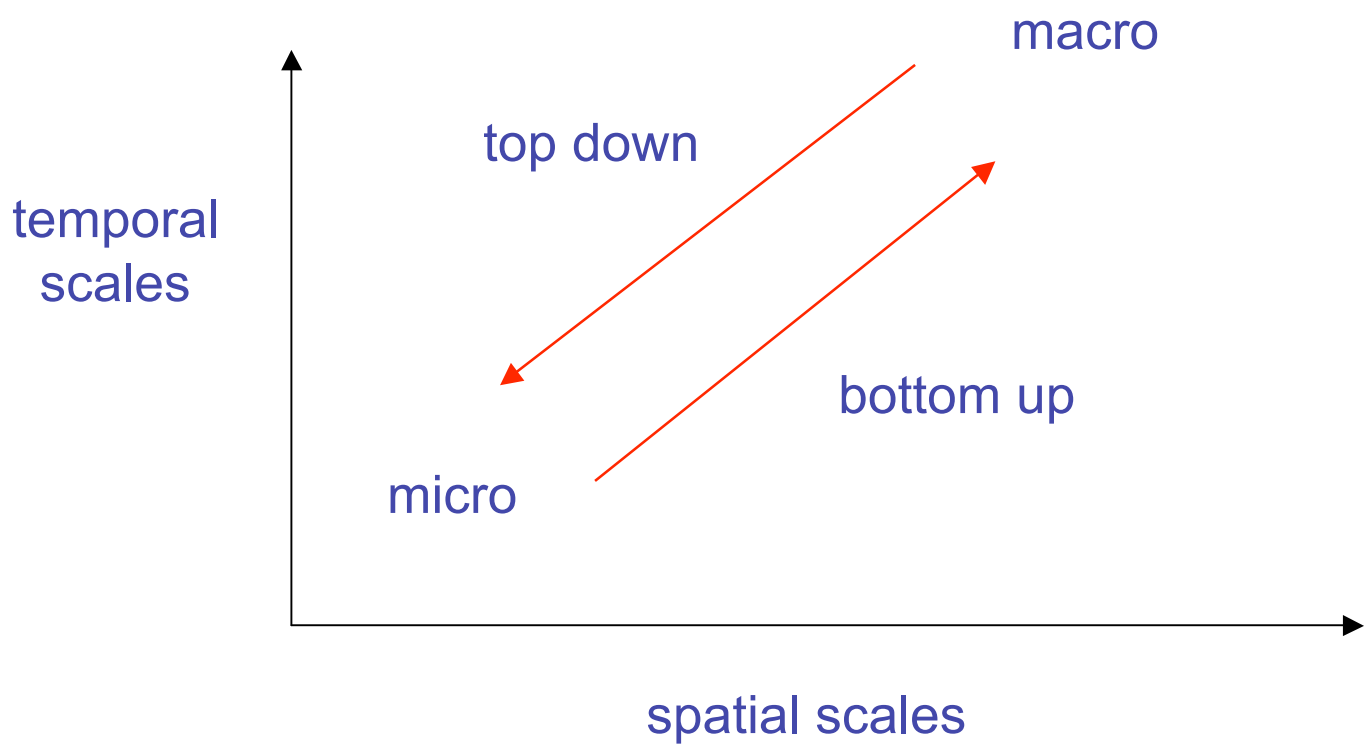

The challenge of multi-scale computing

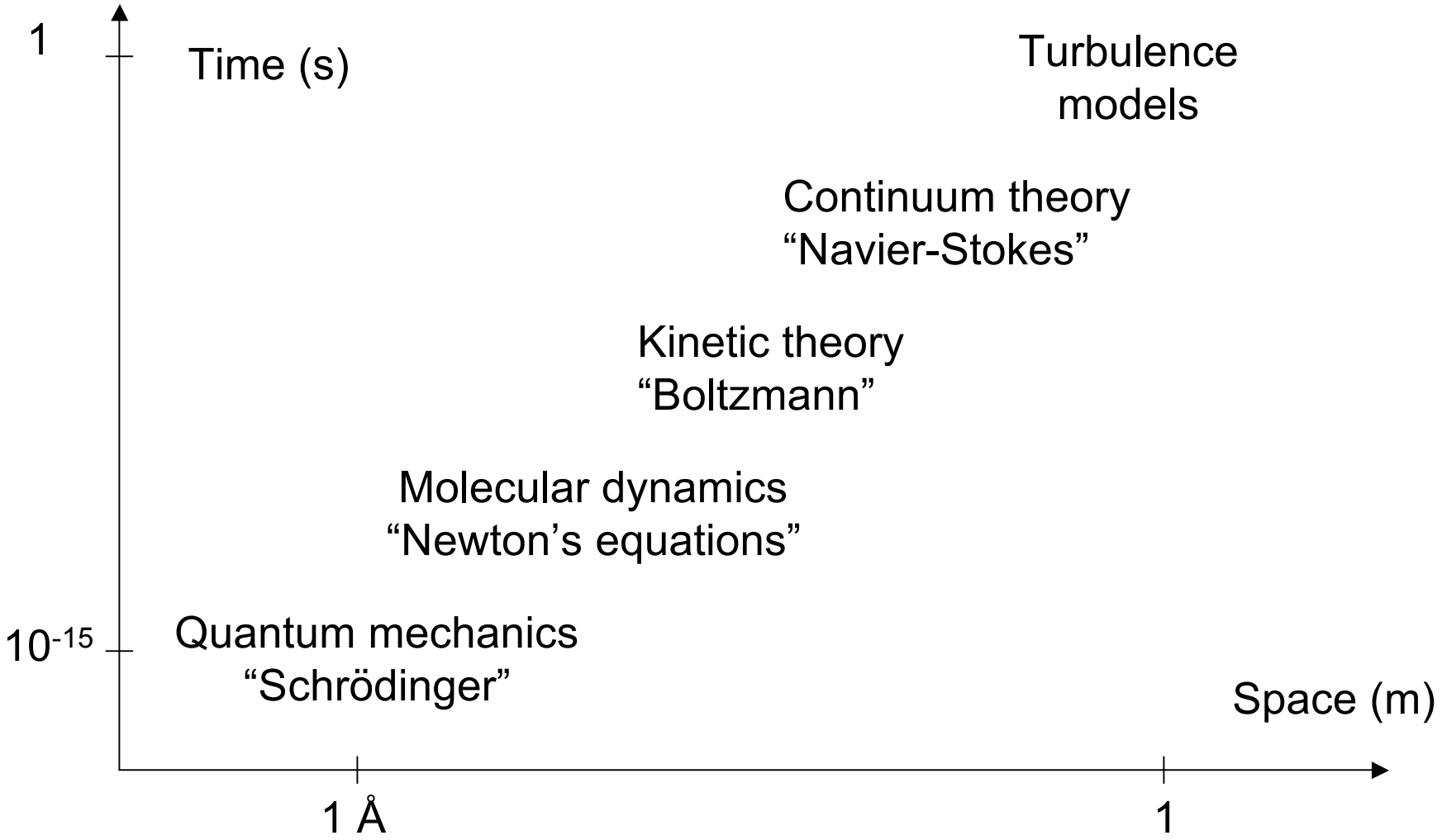

Top down or bottom up

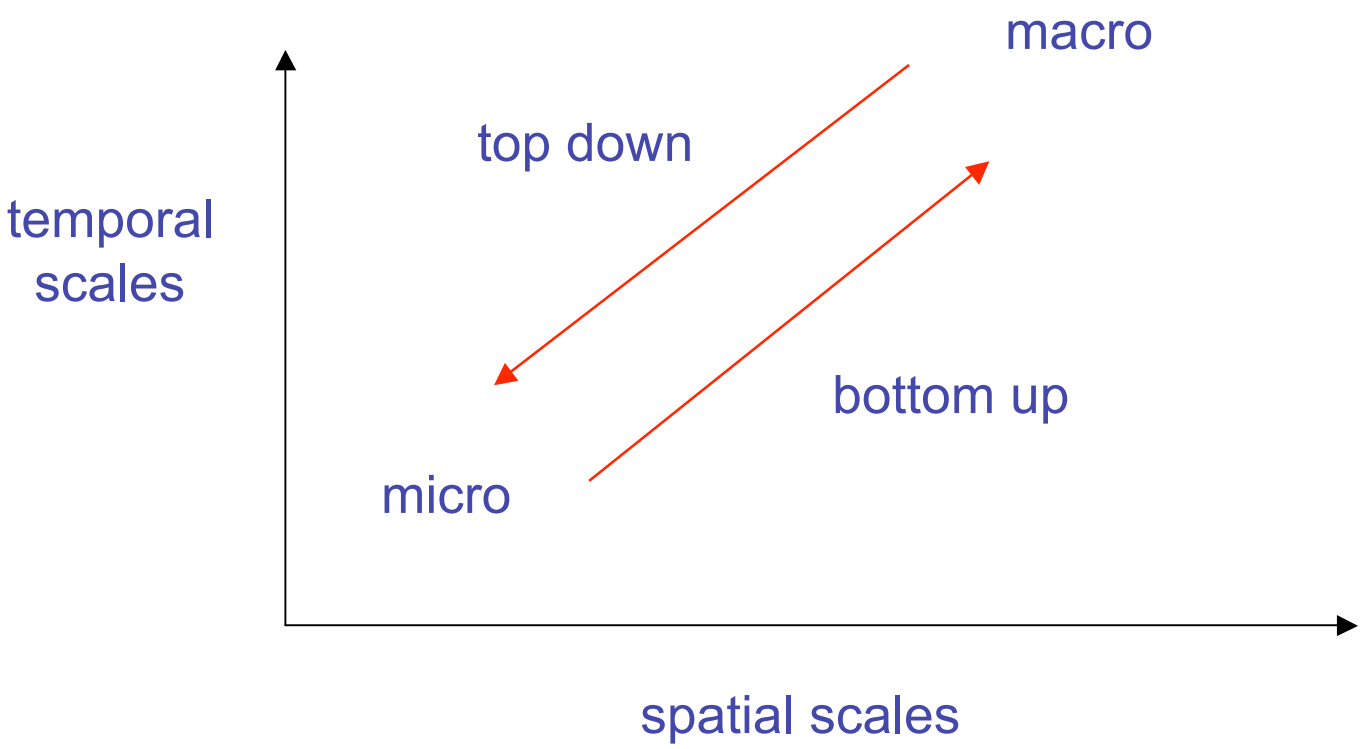

- Top down (standard):
  - Model based on known physics, created for scales and variables of interest, unknown quantities measured
  - The quantities can also be pre-computed from first principles: parameter passing or sequential multi-scale modeling
  - HMM

- Bottom up: aims at directly extending the range of a micro-scale method
  - Examples: Car-Parinello, equation free, accelerated molecular dynamics
  - The quasi continuum method can be seen both ways

Pitfalls of bottom up

- Connecting micro-scale modules without macro-scale understanding
  - Example: extrapolation in time or interpolation in space for the equation free method may lead to instability
  - In general, multi-physics couplings may miss the coupling phenomena. Example interface waves.
- Rescaling introduces scaling error and may miss resonance phenomena

8.5 Choice of macro-scale variables

- Often macro-scale variables are given by the physical situation. Example: moments like mass momentum and energy are natural for a macro-scale model based on kinetic micro-scale simulation.
- Are these variables enough - a basic closure problem.
- Example: consider dynamical systems with highly oscillatory solution
- The macro-scale variables must allow for micro-scale reconstruction that is consistent with the macro scale evolution